

On the motion of a sphere in a Stokes flow parallel to a Brinkman half-space

By E. R. DAMIANO¹, D. S. LONG¹, F. H. EL-KHATIB¹
AND T. M. STACE^{1,2}

¹Department of Mechanical and Industrial Engineering, University of Illinois at Urbana-Champaign, Urbana, IL 61801, USA

²Cavendish Laboratory, University of Cambridge, Cambridge CB3 0HE, UK

(Received 23 October 2002 and in revised form 1 August 2003)

A three-dimensional analysis is presented of the Stokes flow, adjacent to a Brinkman half-space, that is induced or altered by the presence of a sphere in the flow field that (a) translates uniformly without rotating, (b) rotates uniformly without translating, or (c) is fixed in a shear flow that is uniform in the far field. The linear superposition of these three flow regimes is also considered for the special case of the free motion of a neutrally buoyant sphere. Exact solutions to the momentum equations are obtained in terms of infinite series expansions in the Stokes-flow region and in terms of integral transforms in the Brinkman medium. Attention is focused on the approach to the asymptotic limit as the ratio of Newtonian- to Darcy-drag forces vanishes. From the leading-order asymptotic approximations, implicit recursion relations are derived to determine the coefficients in the series solutions such that those solutions exactly satisfy the boundary and interfacial conditions as well as the continuity equations in both the Stokes-flow and Brinkman regions. For each of the three flow regimes considered, results are presented in terms of the drag force on the sphere and torque about the sphere centre as a function of the dimensionless separation distance between the sphere and the interfacial plane for several small values of the dimensionless hydraulic permeability of the Brinkman medium. Finally, the free motion of a neutrally buoyant sphere is found by requiring that the net hydrodynamic drag force and torque acting on the sphere vanish. Results for this case are presented in terms of the dimensionless translational and rotational speeds of the sphere as a function of the dimensionless separation distance for several small values of the dimensionless hydraulic permeability. The work is motivated by its potential application as an analytical tool in the study of near-wall microfluidics in the vicinity of the glycocalyx surface layer on vascular endothelium and in microelectromechanical systems devices where charged macromolecules may become adsorbed to microchannel walls.

1. Introduction

Numerous studies have been undertaken over the years into the hydrodynamic interactions that arise in a Stokes flow between a rigid solid of revolution and another object, such as a plane of infinite extent. One of the earliest of such studies (Jeffery 1915) employed bispherical coordinates to solve the symmetrical problem of solids of revolution that are rotating about an axis perpendicular to a plane boundary. Stimson & Jeffery (1926) determined, using bispherical coordinates, the motion of a viscous fluid that is caused by two spheres, of equal or unequal size,

translating at a constant relative speed along the axis passing through the centres of both spheres. The problem of a Stokes flow induced by the motion of a sphere near a smooth plane under (a) pure rotation without translation, and (b) uniform translation without rotation, has been solved exactly in terms of series solutions by Dean & O'Neill (1963)[†] and O'Neill (1964), respectively. Their analyses also used a bispherical coordinate system, which, when combined with a decomposition of the velocity field, led to closed-form infinite series solutions for the velocity and pressure fields. Using these solutions, the net hydrodynamic drag force on the sphere and the net torque about the sphere centre were obtained analytically in terms of series expansions from direct surface integrations of the velocity field. Since the governing differential equations and boundary conditions are linear, the solutions to these two cases, together with the solution to the problem of a uniform shear flow around a stationary sphere near a plane wall (Goldman 1966; Goren & O'Neill 1971), can be linearly superposed to provide the solution to the more complicated problem of a translating, rotating sphere parallel to a plane wall in a uniform shear flow. For neutrally buoyant spheres, the net hydrodynamic force and torque about the sphere centre must vanish. Goldman, Cox & Brenner (1967*b*) followed this approach to obtain the translational and rotational speeds of the sphere as a function of the dimensionless separation distance between the sphere and the plane.

The hydrodynamic interaction with bodies of revolution that are in the presence of a permeable medium has also been given considerable attention over the years (Brinkman 1947; Kim & Russel 1985; O'Neill & Bhatt 1991; Davis & Stone 1993; Solomentsev & Anderson 1996; Feng, Ganatos, & Weinbaum 1998*a, b*; Broday 2002). In most of these studies, the porous medium was modelled using the Brinkman equation (Brinkman 1947), which has been shown on theoretical grounds to be relevant when a viscous fluid flows through a cloud of spherical particles or through random arrays of spheres or parallel circular posts (Tam 1969; Lundgren 1972; Howells 1974). The Brinkman equation is applicable in this context when the particles collectively occupy negligible volume and are each small relative to length scales that are characteristic of the flow (Brinkman 1947; Tam 1969; Saffman 1971; Lundgren 1972; Howells 1974). In such flows, the Newtonian viscous drag forces, arising from velocity gradients in the flow, and Darcy drag forces, arising from permeation-induced viscous drag of flow through the particles, together balance the pressure gradient. Typically, the Darcy drag forces dominate except near solid boundaries and fluid interfaces where Newtonian viscous forces become important (Hou *et al.* 1989).

A straightforward generalization of the Brinkman medium, to a rigid porous material having a non-vanishing solid volume fraction, can be achieved using continuum mechanics of heterogeneous materials for binary mixtures (Truesdell & Toupin 1960). The conservation equations and interfacial velocity and stress conditions arising from the mixture theory are similar in form to those that arise for a Brinkman medium (Truesdell & Toupin 1960; Saffman 1971; Hou *et al.* 1989); however two additional parameters appear: the solid volume fraction, ϕ^s , and viscosity, μ^f , of the fluid constituent in the porous medium. The difficulty inherent in this more general approach emerges when a quantitative estimate of μ^f is needed, as this quantity is

[†] Although the results of Dean & O'Neill (1963) contained a computational error, their analysis has since been found to be correct (Goldman, Cox & Brenner 1967*a*). Our analysis corroborates this finding.

not simply equivalent to the viscosity of the fluid constituent when separated from the porous medium. It is only in the limit of a vanishing solid volume fraction, i.e. as $\phi^s \rightarrow 0$, that the viscosities of the fluid constituent inside and outside the porous medium converge (Truesdell & Toupin 1960).

In the present study, we solve the problem of a sphere in a Stokes flow translating parallel to the bounding plane of a Brinkman half-space and rotating about an axis that is parallel to that plane and perpendicular to the direction of translation. Exact solutions, which satisfy the governing momentum equations for the velocity field and Laplace's equation for the pressure, are obtained in the Stokes-flow region above the plane in terms of infinite series expansions involving Legendre polynomials and associated Legendre polynomials, and in the Brinkman medium below the plane in terms of generalized integer-order Hankel (or Fourier–Bessel) transform integrals. Continuity of the velocity and stress-traction vectors across the interfacial plane separating the Stokes-flow and Brinkman regions is imposed, together with the no-slip boundary condition on the sphere surface, for each of three flow regimes. Attention is focused on the approach to the asymptotic limit as the ratio of Darcy- to Newtonian-drag forces vanishes. This asymptotic parameter, which we refer to as the dimensionless hydraulic permeability of the Brinkman medium, in essence characterizes the ratio of viscous drag forces associated with fluid-velocity gradients in the Brinkman medium to permeation-induced viscous drag forces associated with fluid motion relative to the solid constituent of the Brinkman medium. From the leading-order asymptotic approximation of the integral-transform solutions, implicit recursion relations are derived to determine the coefficients in the series solutions such that those solutions exactly satisfy the boundary and interfacial conditions as well as the continuity equations in both the Stokes-flow and Brinkman regions. The significant solution that is obtained, therefore, exactly satisfies the momentum equations associated with the Stokes-flow region, asymptotically satisfies the momentum equations associated with the Brinkman medium, and exactly satisfies Laplace's equation for the pressure everywhere. Solutions are obtained for the following three flow regimes: (a) a Stokes flow of an otherwise quiescent fluid that is induced by the uniform translation of a sphere through the fluid with the sphere centre maintained at a constant distance, d , from the bounding plane of a Brinkman half-space; (b) a Stokes flow of an otherwise quiescent fluid that is induced by the pure rotation of a sphere in that fluid about an axis parallel to the bounding plane of a Brinkman half-space and at a distance d from that plane; and (c) a Stokes flow around a stationary sphere with its centre located a distance d from the bounding plane of a Brinkman half-space where the far-field flow is a uniform shear field having a velocity that increases linearly with increasing distance from the plane into the Stokes-flow region. Finally, a particular linear superposition of these three solutions is obtained to find the free motion of a neutrally buoyant sphere in a uniform shear field where the sphere centre translates parallel to and at a distance d from the bounding plane of a Brinkman half-space.

A primary motivation for this work is its potential application to blood flow in the microcirculation and, in particular, to a dilute, macromolecular, carbohydrate-rich surface layer on the vascular endothelium known as the glycocalyx. Recent studies in capillaries and venules estimate the thickness of the glycocalyx *in vivo* to be $\sim 0.3\text{--}0.5\ \mu\text{m}$ (Vink & Duling 1996; Smith *et al.* 2003). Based on results of the analysis presented here, microfluidic studies near the vessel wall using high-resolution intravital fluorescent micro-particle image velocimetry in post-capillary venules have revealed nearly complete retardation of plasma flow through the glycocalyx and

provide the first direct evidence for a hydrodynamically relevant surface layer on vascular endothelium (Smith *et al.* 2003).

2. General formulation

For a Stokes flow of a fluid having constant viscosity, μ , adjacent to a slow steady divergent-free flow in a Brinkman half-space also having constant viscosity, μ , and constant hydraulic resistivity, K , the mass and momentum conservation equations are given by

$$-\mu \nabla \times \nabla \times \tilde{\mathbf{v}}^* = \nabla \tilde{p}^*, \quad \nabla \cdot \tilde{\mathbf{v}}^* = 0, \quad (2.1)$$

$$-\mu \nabla \times \nabla \times \mathbf{v}^* - K \mathbf{v}^* = \nabla p^*, \quad \nabla \cdot \mathbf{v}^* = 0, \quad (2.2)$$

where $\tilde{\mathbf{v}}^*$ and \mathbf{v}^* are the dimensional fluid velocity vectors and \tilde{p}^* and p^* denote the dimensional pressure fields, in the Stokes-flow and Brinkman regions, respectively (variables that carry a tilde are associated with the Stokes-flow region). Taking the divergence of the momentum equations and using the fact that both velocity fields are solenoidal, it follows that $\nabla \cdot \nabla \tilde{p}^* = \nabla^2 \tilde{p}^* = 0$ and $\nabla \cdot \nabla p^* = \nabla^2 p^* = 0$ throughout their respective fields.

3. Brinkman equations in cylindrical coordinates

We consider adjacent Stokes-flow and Brinkman half-spaces that share a common planar interface, denoted by P , at $z^* = 0$ in Cartesian coordinates (x^*, y^*, z^*) where the fluid velocity vector in the Brinkman medium is given by $\mathbf{v}^* = v_x^* \mathbf{e}_x + v_y^* \mathbf{e}_y + v_z^* \mathbf{e}_z$. In cylindrical coordinates (r^*, θ, z^*) , where $x^* = r^* \cos \theta$, $y^* = r^* \sin \theta$, and $\mathbf{v}^* = v_r^* \mathbf{e}_r + v_\theta^* \mathbf{e}_\theta + v_z^* \mathbf{e}_z$, the governing conservation equations in the Brinkman medium, given by (2.2), take the form

$$\nabla^2 v_r^* - \frac{v_r^*}{r^{*2}} - \frac{2}{r^{*2}} \frac{\partial v_\theta^*}{\partial \theta} - \frac{K}{\mu} v_r^* = \frac{1}{\mu} \frac{\partial p^*}{\partial r^*}, \quad (3.1)$$

$$\nabla^2 v_\theta^* - \frac{v_\theta^*}{r^{*2}} + \frac{2}{r^{*2}} \frac{\partial v_r^*}{\partial \theta} - \frac{K}{\mu} v_\theta^* = \frac{1}{\mu r^*} \frac{\partial p^*}{\partial \theta}, \quad (3.2)$$

$$\nabla^2 v_z^* - \frac{K}{\mu} v_z^* = \frac{1}{\mu} \frac{\partial p^*}{\partial z^*}, \quad (3.3)$$

$$\frac{\partial v_r^*}{\partial r^*} + \frac{v_r^*}{r^*} + \frac{1}{r^*} \frac{\partial v_\theta^*}{\partial \theta} + \frac{\partial v_z^*}{\partial z^*} = 0 \quad (3.4)$$

where the scalar Laplacian is defined as

$$\nabla^2 = \frac{\partial^2}{\partial r^{*2}} + \frac{1}{r^*} \frac{\partial}{\partial r^*} + \frac{1}{r^{*2}} \frac{\partial^2}{\partial \theta^2} + \frac{\partial^2}{\partial z^{*2}}.$$

Following the approach of Dean & O'Neill (1963), we note that, in cylindrical coordinates, the θ -dependence can be eliminated from the problem and a useful decoupling occurs if p^* and the cylindrical components of \mathbf{v}^* are written as

$$p^* = \frac{\mu V}{c} Q(r, z) \cos \theta, \quad v_r^* = \frac{1}{2} V (r Q(r, z) + U_0(r, z) + U_2(r, z)) \cos \theta, \quad (3.5)$$

$$v_\theta^* = \frac{1}{2} V (U_2(r, z) - U_0(r, z)) \sin \theta, \quad v_z^* = \frac{1}{2} V (z Q(r, z) + 2w(r, z)) \cos \theta, \quad (3.6)$$

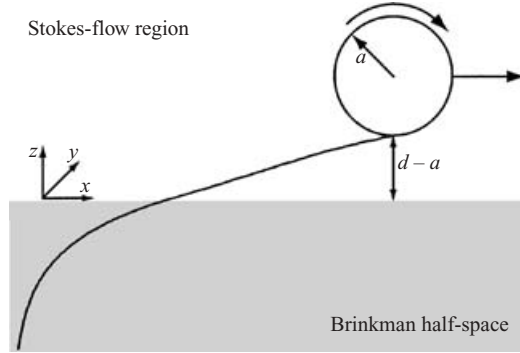


FIGURE 1. Schematic depicting the fluid velocity profile arising from the translational and rotational motion of a sphere in a Stokes flow adjacent to a Brinkman half-space.

where V is a characteristic velocity, $r = r^*/c$, and $z = z^*/c$. For a sphere of radius a in the Stokes-flow region, the characteristic length scale $c = (d^2 - a^2)^{1/2}$, where d is the distance between the sphere centre and interfacial plane, P (see figure 1). It is convenient to choose c as our characteristic length scale since this will render the transformation that we will introduce below, between dimensionless cylindrical coordinates and bispherical coordinates, free of parameters. This, in turn, will simplify the form of many expressions we will derive that will use the bispherical coordinate system.

When (3.5) and (3.6) are substituted into the conservation equations, the fully three-dimensional problem reduces to one that is dependent only on the variables r and z . In particular, (3.1)–(3.4) and Laplace’s equation for the pressure are satisfied if

$$L_1^2 Q = 0, \quad L_1^2 w - \epsilon^{-2} (w + \frac{1}{2}zQ) = 0, \quad (3.7)$$

$$L_0^2 U_0 - \epsilon^{-2} (U_0 + \frac{1}{2}rQ) = 0, \quad L_2^2 U_2 - \epsilon^{-2} (U_2 + \frac{1}{2}rQ) = 0, \quad (3.8)$$

$$\left(3 + r \frac{\partial}{\partial r} + z \frac{\partial}{\partial z}\right) Q + \frac{\partial U_0}{\partial r} + \left(\frac{\partial}{\partial r} + \frac{2}{r}\right) U_2 + 2 \frac{\partial w}{\partial z} = 0, \quad (3.9)$$

where

$$L_m^2 = \frac{\partial^2}{\partial r^2} + \frac{1}{r} \frac{\partial}{\partial r} - \frac{m^2}{r^2} + \frac{\partial^2}{\partial z^2}.$$

In (3.7) and (3.8), $\epsilon^2 = \mu/(Kc^2)$ is the dimensionless hydraulic permeability of the Brinkman medium. Based on simple dimensional arguments, one can show from (2.2) that $\epsilon^2 = \mu V c^{-2}/(KV)$, which characterizes the ratio of viscous drag forces associated with fluid-velocity gradients in the Brinkman medium to permeation-induced viscous drag forces associated with fluid motion relative to the solid constituent of the Brinkman medium. Note that in the limit as $\epsilon \rightarrow 0$, the interfacial plane, P , becomes an impermeable boundary. The cylindrical-coordinate representation of the equations associated with the Stokes-flow region are given by (3.1)–(3.9) when K and ϵ^{-2} vanish, and tildes are added to all dependent variables.

4. Stokes equations in bispherical coordinates

Due to the presence of the sphere in the Stokes-flow region, cylindrical coordinates are not an ideal choice. On the other hand, since the interfacial plane, P , is a degenerate sphere in the limit of infinite radius of curvature, it is convenient to

express the cylindrical components of the velocity field in the Stokes-flow region in bispherical coordinates (η, ξ) , which are related to r and z according to

$$r = \frac{\sin \eta}{\cosh \xi - \cos \eta}, \quad z = \frac{\sinh \xi}{\cosh \xi - \cos \eta} \quad (0 \leq \eta \leq \pi, 0 \leq \xi \leq \alpha). \quad (4.1)$$

The coordinate surface $\xi = \alpha > 0$ corresponds to the locus of points that lie on the sphere surface, S , while the coordinate surface $\xi = z = 0$ corresponds to the locus of points that lie on the interfacial plane, P , which is the only coordinate surface that the cylindrical and bispherical coordinate systems share. Using the chain rule to express r - and z -derivatives and the differential operator L_m^2 in terms of the bispherical coordinates, η and ξ , the Stokes equations are satisfied if

$$\mathcal{L}_1^2 \tilde{Q} = \mathcal{L}_1^2 \tilde{w} = \mathcal{L}_0^2 \tilde{U}_0 = \mathcal{L}_2^2 \tilde{U}_2 = 0 \quad (4.2)$$

and

$$3\tilde{Q} + 2\operatorname{cosec} \eta (\cosh \xi - \cos \eta) \tilde{U}_2 - \cos \eta \sinh \xi \frac{\partial \tilde{Q}}{\partial \xi} - \sin \eta \cosh \xi \frac{\partial \tilde{Q}}{\partial \eta} \\ - (1 - \cos \eta \cosh \xi) \left(\frac{\partial \tilde{U}_0}{\partial \eta} + \frac{\partial \tilde{U}_2}{\partial \eta} - 2 \frac{\partial \tilde{w}}{\partial \xi} \right) - \sin \eta \sinh \xi \left(\frac{\partial \tilde{U}_0}{\partial \xi} + \frac{\partial \tilde{U}_2}{\partial \xi} + 2 \frac{\partial \tilde{w}}{\partial \eta} \right) = 0, \quad (4.3)$$

where

$$\mathcal{L}_m^2 = \frac{\partial^2}{\partial \eta^2} + \frac{\partial^2}{\partial \xi^2} + \frac{1 - \cos \eta \cosh \xi}{\sin \eta (\cos \eta - \cosh \xi)} \frac{\partial}{\partial \eta} + \frac{\sinh \xi}{\cos \eta - \cosh \xi} \frac{\partial}{\partial \xi} - \frac{m^2}{\sin^2 \eta}. \quad (4.4)$$

For the case of pure translation of a sphere through an otherwise quiescent fluid, the characteristic velocity is taken to be $V = U$, the sphere translational speed, whereas for pure rotation of a sphere through an otherwise quiescent fluid, $V = c\Omega$, where Ω is the sphere rotational speed. For the case of a stationary sphere in an otherwise uniform shear field within the Stokes-flow region, the characteristic velocity is taken to be $V = c\dot{\gamma}$, where $\dot{\gamma}$ characterizes the strength of the shear field.

Whereas in the case of the purely translating or purely rotating sphere, the fluid velocity decays to zero in the far field, in the case of the stationary sphere, the far-field solution in the Stokes-flow region is given by

$$\tilde{\mathbf{v}}(\mathbf{x} \rightarrow \infty) = c\dot{\gamma}(z + \epsilon)\mathbf{e}_x, \quad \forall z \geq 0$$

and in cylindrical coordinates by

$$\tilde{\mathbf{v}}(r \rightarrow \infty, \theta, z) = c\dot{\gamma}(z + \epsilon)(\cos \theta \mathbf{e}_r - \sin \theta \mathbf{e}_\theta), \quad \forall z \geq 0. \quad (4.5)$$

In the far field of the Brinkman medium, the velocity decays exponentially in magnitude according to $c\dot{\gamma}\epsilon e^{z/\epsilon}$, $\forall z \leq 0$, where $c\dot{\gamma}\epsilon$ is the magnitude of the far-field slip velocity on the interfacial plane, P . This result is consistent with the slip velocity given in the classic works of Beavers & Joseph (1967) and Taylor (1971) at the interface between a porous medium and a Newtonian fluid subjected to a linear shear field. Adding the far-field solution given by (4.5) to the velocity field given by (3.5) and (3.6), the radial and azimuthal velocity components for the case of a stationary sphere are given by

$$\tilde{v}_r^* = \frac{1}{2}c\dot{\gamma}(r\tilde{Q}(r, z) + \tilde{U}_0(r, z) + \tilde{U}_2(r, z) + 2(z + \epsilon)) \cos \theta, \quad (4.6)$$

$$\tilde{v}_\theta^* = \frac{1}{2}c\dot{\gamma}(\tilde{U}_2(r, z) - \tilde{U}_0(r, z) - 2(z + \epsilon)) \sin \theta. \quad (4.7)$$

Since adding to $\tilde{v}_r^*/\cos\theta$ and subtracting from $\tilde{v}_\theta^*/\sin\theta$ the same affine function of z does not change the left-hand sides of (3.1) or (3.2) when $K=0$, the differential equations governing \tilde{Q} , \tilde{w} , \tilde{U}_0 , and \tilde{U}_2 , for the case of a stationary sphere in an otherwise uniform shear field within the Stokes-flow region, are still given by (4.2)–(4.4).

5. Exact solution of the governing equations

Below we provide general forms of the exact solutions to (3.7), (3.8), and (4.2) and the conditions under which those solutions can be made to satisfy the continuity equations given by (3.9) and (4.3).

5.1. Solution in the Brinkman region

The exact solution to (3.7) and (3.8) can be expressed in terms of generalized Hankel integral transforms. From the solution to Q , one finds that the complementary and particular solutions for w , U_0 , and U_2 are given on $r \geq 0$ and $z \leq 0$, to within the arbitrary functions $A(s)$, $C(s)$, $E(s)$, and $G(s)$, by

$$w(r, z) = -\frac{1}{2}zQ - \epsilon^2 \frac{\partial Q}{\partial z} + \int_0^\infty \epsilon A(s) \exp((s^2 + \epsilon^{-2})^{1/2}z) J_1(sr) s \, ds, \quad (5.1)$$

$$U_0(r, z) = -\frac{1}{2}rQ - \epsilon^2 \left(\frac{\partial Q}{\partial r} + \frac{Q}{r} \right) + \int_0^\infty \epsilon E(s) \exp((s^2 + \epsilon^{-2})^{1/2}z) J_0(sr) s \, ds, \quad (5.2)$$

$$U_2(r, z) = -\frac{1}{2}rQ - \epsilon^2 \left(\frac{\partial Q}{\partial r} - \frac{Q}{r} \right) + \int_0^\infty \epsilon G(s) \exp((s^2 + \epsilon^{-2})^{1/2}z) J_2(sr) s \, ds, \quad (5.3)$$

where

$$Q(r, z) = \int_0^\infty \epsilon C(s) e^{sz} J_1(sr) s \, ds \quad (5.4)$$

and J_0 , J_1 , and J_2 are, respectively, the zeroth-, first-, and second-order Bessel functions of the first kind. Note that e^{-sz} , corresponding to the second linearly independent complementary solution associated with Q , and $\exp(-(s^2 + \epsilon^{-2})^{1/2}z)$, corresponding to the second linearly independent complementary solution associated with w , U_0 , and U_2 , grow without bound in the Brinkman half-space, since $z \leq 0$, and are therefore not admissible.

Substituting (5.1)–(5.4) into the continuity equation, given by (3.9), and using the recursion relations for the Bessel functions, one obtains a solenoidal velocity field throughout the Brinkman medium if

$$2(s^2 + \epsilon^{-2})^{1/2}A(s) - s(E(s) - G(s)) = 0. \quad (5.5)$$

With $A(s)$ determined from (5.5), only $C(s)$, $E(s)$, and $G(s)$ remain to be determined in order to fully specify the solution in the Brinkman medium.

5.2. Solution in the Stokes-flow region

Series solutions provided by Dean & O'Neill (1963) that exactly satisfy (4.2) are given by

$$\tilde{Q}(\eta, \xi) = \sin \eta (\cosh \xi - \nu)^{1/2} \sum_{n=1}^{\infty} \left(c_n \cosh \left(n + \frac{1}{2} \right) \xi + d_n \sinh \left(n + \frac{1}{2} \right) \xi \right) P'_n(\nu), \quad (5.6)$$

$$\tilde{w}(\eta, \xi) = \sin \eta (\cosh \xi - \nu)^{1/2} \sum_{n=1}^{\infty} \left(a_n \cosh \left(n + \frac{1}{2} \right) \xi + b_n \sinh \left(n + \frac{1}{2} \right) \xi \right) P'_n(\nu), \quad (5.7)$$

$$\tilde{U}_0(\eta, \xi) = (\cosh \xi - \nu)^{1/2} \sum_{n=0}^{\infty} \left(e_n \cosh \left(n + \frac{1}{2} \right) \xi + f_n \sinh \left(n + \frac{1}{2} \right) \xi \right) P_n(\nu), \quad (5.8)$$

$$\tilde{U}_2(\eta, \xi) = \sin^2 \eta (\cosh \xi - \nu)^{1/2} \sum_{n=2}^{\infty} \left(g_n \cosh \left(n + \frac{1}{2} \right) \xi + h_n \sinh \left(n + \frac{1}{2} \right) \xi \right) P''_n(\nu), \quad (5.9)$$

where P_n are the Legendre polynomials of the first kind, $\nu = \cos \eta$, and the primes denote differentiation with respect to ν .

Substituting this solution into the continuity equation, given by (4.3), and using the recursion relations for the Legendre polynomials, one obtains a solenoidal velocity field throughout the Stokes-flow region if

$$\begin{aligned} \frac{5}{2}d_n - \frac{1}{2}((n-1)d_{n-1} - (n+2)d_{n+1}) - \frac{1}{2}(f_{n-1} - 2f_n + f_{n+1}) \\ + \frac{1}{2}((n-2)(n-1)h_{n-1} - 2(n-1)(n+2)h_n + (n+2)(n+3)h_{n+1}) \\ - (n-1)a_{n-1} + (2n+1)a_n - (n+2)a_{n+1} = 0, \quad n = 1, 2, \dots \end{aligned} \quad (5.10)$$

and

$$\begin{aligned} \frac{5}{2}c_n - \frac{1}{2}((n-1)c_{n-1} - (n+2)c_{n+1}) - \frac{1}{2}(e_{n-1} - 2e_n + e_{n+1}) \\ + \frac{1}{2}((n-2)(n-1)g_{n-1} - 2(n-1)(n+2)g_n + (n+2)(n+3)g_{n+1}) \\ - (n-1)b_{n-1} + (2n+1)b_n - (n+2)b_{n+1} = 0, \quad n = 1, 2, \dots \end{aligned} \quad (5.11)$$

6. Boundary conditions on the sphere

The boundary conditions on the sphere surface for the three elemental problems we will consider are written in bispherical coordinates below in terms of the variables \tilde{Q} , \tilde{w} , \tilde{U}_0 , and \tilde{U}_2 . A linear superposition of the solutions to these three problems will subsequently be obtained for the particular case of the free motion of a neutrally buoyant sphere in a uniform shear field.

6.1. Pure translation

For pure steady translation of a sphere parallel to the plane, P , with linear velocity $U \mathbf{e}_x$ in the positive x -direction, the no-slip boundary condition on the sphere surface, S , is given by

$$\tilde{\mathbf{v}}(\mathbf{x}) = U \mathbf{e}_x, \quad \forall \mathbf{x} \in S. \quad (6.1)$$

In cylindrical coordinates this boundary condition takes the form

$$\tilde{\mathbf{v}}(r, \theta, z) = U(\cos \theta \mathbf{e}_r - \sin \theta \mathbf{e}_\theta), \quad \forall (r, \theta, z) \in S. \quad (6.2)$$

Using (3.5) and (3.6) in the left-hand side, we find that (6.2) is satisfied if

$$\tilde{U}_0(r, z) - 2 = \tilde{U}_2(r, z) = -\frac{1}{2}r \tilde{Q}(r, z), \quad r \tilde{w}(r, z) = z \tilde{U}_2(r, z), \quad \forall (r, z) \in S. \quad (6.3)$$

In bispherical coordinates, where the sphere surface, S , corresponds to the coordinate surface $\xi = \alpha$, these conditions are given by

$$\tilde{U}_0(\eta, \alpha) - 2 = \tilde{U}_2(\eta, \alpha) = -\frac{\tilde{Q}(\eta, \alpha) \sin \eta}{2(\cosh \alpha - \cos \eta)}, \quad \sin \eta \tilde{w}(\eta, \alpha) = \sinh \alpha \tilde{U}_2(\eta, \alpha). \quad (6.4)$$

Making use of the recursion relations for the Legendre polynomials, three recursion relations for this boundary condition can be obtained by substituting the series solutions given by (5.6)–(5.9) into (6.4). The recursion relations derived from these conditions are given in Appendix A, § A.1.

6.2. Pure rotation

For pure steady rotation of a sphere about an axis parallel to the plane, P , with angular velocity $\Omega \mathbf{e}_y$ in the positive y -direction, the no-slip boundary condition on the sphere surface, S , is given by

$$\tilde{\mathbf{v}}(\mathbf{x}) = \Omega \mathbf{e}_y \times \mathbf{r}_s, \quad \forall \mathbf{x} \in S, \quad (6.5)$$

where \mathbf{r}_s is the position vector originating from the sphere centre to any point on the sphere surface. In Cartesian and cylindrical coordinates, this boundary condition takes the form

$$\tilde{\mathbf{v}}(x, y, z) = c \Omega ((z - d/c) \mathbf{e}_x - x \mathbf{e}_z), \quad \forall (x, y, z) \in S,$$

$$\tilde{\mathbf{v}}(r, \theta, z) = c \Omega ((z - d/c)(\cos \theta \mathbf{e}_r - \sin \theta \mathbf{e}_\theta) - r \cos \theta \mathbf{e}_z), \quad \forall (r, \theta, z) \in S, \quad (6.6)$$

where d is the distance from the plane to the centre of the sphere located at $\mathbf{x} = d \mathbf{e}_z$. Using (3.5) and (3.6) in the left-hand side, we find that (6.6) is satisfied if

$$\tilde{U}_0(r, z) - 2(z - d/c) = \tilde{U}_2(r, z) = -\frac{1}{2}r \tilde{Q}(r, z), \quad \forall (r, z) \in S, \quad (6.7)$$

$$r(\tilde{w}(r, z) + r) = z \tilde{U}_2(r, z), \quad \forall (r, z) \in S. \quad (6.8)$$

In bispherical coordinates, where the sphere surface, S , corresponds to the coordinate surface $\xi = \alpha$, these conditions are given by

$$\tilde{U}_0(\eta, \alpha) - \frac{2 \sinh \alpha}{\cosh \alpha - \cos \eta} + 2 \coth \alpha = \tilde{U}_2(\eta, \alpha) = -\frac{\tilde{Q}(\eta, \alpha) \sin \eta}{2(\cosh \alpha - \cos \eta)}, \quad (6.9)$$

$$\sin \eta \tilde{w}(\eta, \alpha) + \frac{\sin^2 \eta}{\cosh \alpha - \cos \eta} = \sinh \alpha \tilde{U}_2(\eta, \alpha), \quad (6.10)$$

where we have made use of the geometric relationship $d/c = \coth \alpha$ (Dean & O'Neill 1963). The recursion relations derived from these conditions are given in Appendix A, § A.2.

6.3. Uniform shear

For a stationary sphere near the plane, P , in a velocity field that varies linearly with z in the far field according to (4.5), the no-slip boundary condition on the sphere surface, S , is given by $\tilde{\mathbf{v}}(\mathbf{x}) = \mathbf{0}$, $\forall \mathbf{x} \in S$. From (4.6), (4.7), and the second of (3.6), we find that this condition is satisfied if

$$\tilde{U}_0(r, z) + 2(z + b) = \tilde{U}_2(r, z) = -\frac{1}{2}r \tilde{Q}(r, z), \quad r \tilde{w}(r, z) = z \tilde{U}_2(r, z), \quad \forall (r, z) \in S. \quad (6.11)$$

In bispherical coordinates, where the sphere surface, S , corresponds to the coordinate surface $\xi = \alpha$, these conditions are given by

$$\tilde{U}_0(\eta, \alpha) + \frac{2 \sinh \alpha}{\cosh \alpha - \cos \eta} + 2 \epsilon = \tilde{U}_2(\eta, \alpha) = -\frac{\tilde{Q}(\eta, \alpha) \sin \eta}{2(\cosh \alpha - \cos \eta)}, \quad (6.12)$$

$$\sin \eta \tilde{w}(\eta, \alpha) = \sinh \alpha \tilde{U}_2(\eta, \alpha). \quad (6.13)$$

The recursion relations derived from these conditions are given in Appendix A, § A.3.

7. Interfacial velocity and stress conditions

We require that the velocity vector and Cauchy stress tensor be continuous across the interfacial plane, P , separating the Stokes-flow region and Brinkman half-space. In particular, if the stress traction vector acting on a plane perpendicular to a unit vector, \mathbf{n} , is given by $\boldsymbol{\sigma} \cdot \mathbf{n}$, where $\boldsymbol{\sigma}$ is the Cauchy stress tensor, then the interfacial velocity and stress conditions are given by

$$\mathbf{v}(\mathbf{x}) = \tilde{\mathbf{v}}(\mathbf{x}), \quad \boldsymbol{\sigma}(\mathbf{x}) \cdot \mathbf{n} = -\tilde{\boldsymbol{\sigma}}(\mathbf{x}) \cdot \tilde{\mathbf{n}}, \quad \forall \mathbf{x} \in P, \quad (7.1)$$

where $\mathbf{n} = \mathbf{e}_z$ and $\tilde{\mathbf{n}} = -\mathbf{e}_z$ are, respectively, the outward-facing normals to the Brinkman and Stokes-flow regions on P . The second of (7.1) indicates that the stress-traction vectors associated with the Stokes-flow and Brinkman regions acting at any point on P are equal in magnitude and direction but of opposite sense. These interfacial conditions are consistent with those used by Davis & Stone (1993) at the interface between two Brinkman media as well as with those derived by Hou *et al.* (1989) at the interface between a binary mixture and a homogeneous fluid in the limit as the fluid volume fraction approaches unity. Broday (2002) used similar conditions at the interface between two Brinkman media but required that the normal velocities vanish at the interface. Such a restriction, however, is not necessary and is technically justified only in the limit as $\epsilon \rightarrow 0$.

In terms of scalar components, the interfacial conditions given by (7.1) are

$$v_r^* = \tilde{v}_r^*, \quad v_\theta^* = \tilde{v}_\theta^*, \quad v_z^* = \tilde{v}_z^*, \quad \forall (r, \theta) \in z=0, \quad (7.2)$$

$$-p^* + 2\mu \frac{\partial v_z^*}{\partial z^*} = -\tilde{p}^* + 2\mu \frac{\partial \tilde{v}_z^*}{\partial z^*}, \quad \forall (r, \theta) \in z=0, \quad (7.3)$$

$$\frac{\partial v_r^*}{\partial z^*} + \frac{\partial v_z^*}{\partial r^*} = \frac{\partial \tilde{v}_r^*}{\partial z^*} + \frac{\partial \tilde{v}_z^*}{\partial r^*}, \quad \frac{\partial v_\theta^*}{\partial z^*} + \frac{1}{r^*} \frac{\partial v_z^*}{\partial \theta} = \frac{\partial \tilde{v}_\theta^*}{\partial z^*} + \frac{1}{r^*} \frac{\partial \tilde{v}_z^*}{\partial \theta}, \quad \forall (r, \theta) \in z=0. \quad (7.4)$$

Since the three velocity components are continuous across P , all r - and θ -derivatives of the velocity components must also be continuous across P . Thus the interfacial conditions on the two deviatoric stress components given by (7.4) reduce to

$$\left. \frac{\partial v_r^*}{\partial z^*} \right|_{z^*=0} = \left. \frac{\partial \tilde{v}_r^*}{\partial z^*} \right|_{z^*=0}, \quad \left. \frac{\partial v_\theta^*}{\partial z^*} \right|_{z^*=0} = \left. \frac{\partial \tilde{v}_\theta^*}{\partial z^*} \right|_{z^*=0}. \quad (7.5)$$

Evaluating the continuity equation given by (3.4) on each side of P , and imposing the continuity in the velocity components across P , it is evident that

$$\left. \frac{\partial v_z^*}{\partial z^*} \right|_{z^*=0} = \left. \frac{\partial \tilde{v}_z^*}{\partial z^*} \right|_{z^*=0}, \quad (7.6)$$

which implies that the pressure is continuous across P in accordance with the condition on the normal Cauchy stress component given by (7.3). Taking the sum of and difference between $v_r^*/\cos\theta$ and $v_\theta^*/\sin\theta$, and likewise for the two deviatoric stress components, and using the continuity of the pressure across P , the six interfacial velocity and stress conditions given by (7.2)–(7.4) are satisfied if

$$Q = \tilde{Q}, \quad w = \tilde{w}, \quad \forall (r, \theta) \in z=0, \quad (7.7)$$

$$U_0 = \tilde{U}_0, \quad U_2 = \tilde{U}_2, \quad \forall (r, \theta) \in z=0, \quad (7.8)$$

$$\frac{r}{2} \frac{\partial Q}{\partial z} + \frac{\partial U_0}{\partial z} = \frac{r}{2} \frac{\partial \tilde{Q}}{\partial z} + \frac{\partial \tilde{U}_0}{\partial z}, \quad \frac{r}{2} \frac{\partial Q}{\partial z} + \frac{\partial U_2}{\partial z} = \frac{r}{2} \frac{\partial \tilde{Q}}{\partial z} + \frac{\partial \tilde{U}_2}{\partial z}, \quad \forall (r, \theta) \in z=0. \quad (7.9)$$

8. Asymptotic approximation of the Brinkman solution

Although the exact integral forms of the complementary and particular solutions to (3.7) and (3.8) are given by (5.1)–(5.3), the fact that $A(s)$, $E(s)$, and $G(s)$ appear in the complementary solutions multiplied by an s -dependent exponential confounds any attempt at obtaining analytical recursion relations for the series coefficients that identically satisfy the six interfacial velocity and stress conditions derived above. On the other hand, such relations can be obtained if one considers the asymptotic limit of the complementary solutions associated with (5.1)–(5.3) as $\epsilon \rightarrow 0$. As this limit is relevant to a variety of problems to which this analysis might apply, we shall proceed by seeking the asymptotic solution that is formally correct in the limit as $\epsilon \rightarrow 0$.

8.1. Series expansions of the complementary solutions for small ϵ

Expanding the complementary solution associated with w , U_0 , and U_2 , given, respectively, by the last term on each of the right-hand sides of (5.1)–(5.3), in powers of ϵ provides

$$w(r, z) \sim -\frac{1}{2}zQ - \epsilon^2 \frac{\partial Q}{\partial z} + e^{z/\epsilon} \int_0^\infty \epsilon A(s) \exp[\{(\epsilon s)^2/2 - (\epsilon s)^4/8 + \dots\}z/\epsilon] J_1(sr) s \, ds, \quad (8.1)$$

$$U_0(r, z) \sim -\frac{1}{2}rQ - \epsilon^2 \left(\frac{\partial Q}{\partial r} + \frac{Q}{r} \right) + e^{z/\epsilon} \int_0^\infty \epsilon E(s) \exp[\{(\epsilon s)^2/2 - (\epsilon s)^4/8 + \dots\}z/\epsilon] J_0(sr) s \, ds, \quad (8.2)$$

$$U_2(r, z) \sim -\frac{1}{2}rQ - \epsilon^2 \left(\frac{\partial Q}{\partial r} - \frac{Q}{r} \right) + e^{z/\epsilon} \int_0^\infty \epsilon G(s) \exp[\{(\epsilon s)^2/2 - (\epsilon s)^4/8 + \dots\}z/\epsilon] J_2(sr) s \, ds, \quad (8.3)$$

where Q is given by (5.4), which exactly satisfies the first of (3.7). If in each integral the functions $A(s)$, $E(s)$, and $G(s)$ decay rapidly over the width of the Gaussian factor, $\exp(\epsilon s^2 z/2)$, then the Gaussian term and all higher-order terms in ϵ within each integral can be replaced with unity to good approximation. We shall assume this to be true in what follows, and verify it for consistency with the solution we obtain later.

The lowest-order asymptotic solution that can be obtained, and which can be made to satisfy the continuity equation in the Brinkman medium exactly, corresponds to neglecting $O(\epsilon^2)$ terms in each of the particular solutions associated with (8.1)–(8.3) and retaining only the leading-order term in each of the associated complementary solutions. In this case, it becomes convenient to define the $O(1)$ functions† $C_0(r)$, $C_1(r)$, and $C_2(r)$ such that

$$w(r, z) \sim -\frac{1}{2}zQ + \epsilon^2 C_1(r) e^{z/\epsilon}, \quad (8.4)$$

$$U_0(r, z) \sim -\frac{1}{2}rQ + \epsilon C_0(r) e^{z/\epsilon}, \quad U_2(r, z) \sim -\frac{1}{2}rQ + \epsilon C_2(r) e^{z/\epsilon}. \quad (8.5)$$

† Whereas $\tilde{Q}(r, z)$, $\tilde{U}_0(r, z)$, and $\tilde{U}_2(r, z)$ are, in general, $O(1)$ quantities, these functions are all $O(\epsilon)$ when evaluated on the interfacial plane, $z = 0$. Consistent with this asymptotic ordering, $Q(r, z)$, $w(r, z)$, $U_0(r, z)$, and $U_2(r, z)$ are all $O(\epsilon)$.

Substituting (8.4) and (8.5) into the continuity equation, given by (3.9), and eliminating $C_1(r)$ we obtain

$$w(r, z) \sim -\frac{1}{2}zQ - \frac{1}{2}\epsilon^2 \left(C'_0(r) + C'_2(r) + \frac{2C_2(r)}{r} \right) e^{z/\epsilon}. \quad (8.6)$$

Substituting (8.5) and (8.6) into (3.5) and (3.6), the velocity components are given to leading order in ϵ by

$$v_r^* \sim \frac{1}{2}\epsilon V (C_0(r) + C_2(r)) e^{z/\epsilon} \cos \theta, \quad v_\theta^* \sim \frac{1}{2}\epsilon V (C_2(r) - C_0(r)) e^{z/\epsilon} \sin \theta, \quad (8.7)$$

$$v_z^* \sim \frac{1}{2}\epsilon^2 V \left(C'_0(r) + C'_2(r) + \frac{2C_2(r)}{r} \right) e^{z/\epsilon} \cos \theta. \quad (8.8)$$

A boundary layer analysis using a singular perturbation method provides the same asymptotic solutions as those given above up to and including terms of $O(\epsilon)$ in v_r^* and v_θ^* and $O(\epsilon^2)$ in v_z^* . It is evident from the solution of a uniform shear field in the Stokes-flow region, given by (4.5), that the magnitude of the slip velocity on the interfacial plane is $O(\epsilon)$. This is consistent with the leading-order radial and azimuthal components of the velocity field in the Brinkman region given by (8.7). It is further evident, upon substitution of (8.7) and (8.8) into the continuity equation given by (3.4), that the leading-order axial component of the velocity field in the Brinkman region must be $O(\epsilon^2)$, which is consistent with (8.8).

8.2. Imposing interfacial conditions

In order to determine the eight sets of coefficients, $\{a_n, b_n, c_n, d_n, e_{n-1}, f_{n-1}, g_{n+1}, h_{n+1}\}$ for $n = 1, 2, \dots$, and the three functions, $C(s)$, $C_0(r)$, and $C_2(r)$, we must impose the six interfacial velocity and stress conditions in addition to the five recursion relations (three obtained from enforcing the no-slip condition on the sphere surface, and two from imposing the continuity equation in the Stokes-flow region). Below we use the six interfacial conditions to eliminate the unknown functions $C(s)$, $C_0(r)$, and $C_2(r)$, and derive three additional recursion relations for the coefficients.

Substituting (8.5) into (7.8) and using the first of (7.7), $C_0(r)$ and $C_2(r)$ are given in terms of the solution in the Stokes-flow region by

$$C_0(r) = \epsilon^{-1} \left(\frac{1}{2}r \tilde{Q}(r, 0) + \tilde{U}_0(r, 0) \right), \quad C_2(r) = \epsilon^{-1} \left(\frac{1}{2}r \tilde{Q}(r, 0) + \tilde{U}_2(r, 0) \right). \quad (8.9)$$

Similarly, alternative expressions for $C_0(r)$ and $C_2(r)$, given by

$$C_0(r) = \left(\frac{r}{2} \frac{\partial \tilde{Q}}{\partial z} + \frac{\partial \tilde{U}_0}{\partial z} \right)_{z=0}, \quad C_2(r) = \left(\frac{r}{2} \frac{\partial \tilde{Q}}{\partial z} + \frac{\partial \tilde{U}_2}{\partial z} \right)_{z=0}, \quad (8.10)$$

can be obtained by substituting the z -derivatives of U_0 and U_2 from (8.5) into (7.9). By combining (8.9) and (8.10) and eliminating $C_0(r)$ and $C_2(r)$, four of the six interfacial conditions are satisfied if the solution in the Stokes-flow region is constrained to satisfy

$$\frac{1}{2}r \tilde{Q}(r, 0) + \tilde{U}_0(r, 0) = \epsilon \left(\frac{r}{2} \frac{\partial \tilde{Q}}{\partial z} + \frac{\partial \tilde{U}_0}{\partial z} \right)_{z=0} \quad (8.11)$$

and

$$\frac{1}{2}r \tilde{Q}(r, 0) + \tilde{U}_2(r, 0) = \epsilon \left(\frac{r}{2} \frac{\partial \tilde{Q}}{\partial z} + \frac{\partial \tilde{U}_2}{\partial z} \right)_{z=0}. \quad (8.12)$$

Using the expressions for $C_0(r)$ and $C_2(r)$, given by (8.9), in (8.6), the interfacial condition relating w and \tilde{w} given by the second of (7.7) is satisfied if

$$\tilde{w}(r, 0) = -\epsilon \left(\tilde{Q} + \frac{r}{2} \frac{\partial \tilde{Q}}{\partial r} + \frac{1}{2} \left(\frac{\partial \tilde{U}_2}{\partial r} + \frac{\partial \tilde{U}_0}{\partial r} \right) + \frac{\tilde{U}_2}{r} \right)_{z=0}. \quad (8.13)$$

In terms of bispherical coordinates, (8.11)–(8.13) take the form

$$\frac{\sin \eta}{2(1 - \cos \eta)} \tilde{Q}(\eta, 0) + \tilde{U}_0(\eta, 0) = \epsilon \left(\frac{1}{2} \sin \eta \frac{\partial \tilde{Q}}{\partial \xi} + (1 - \cos \eta) \frac{\partial \tilde{U}_0}{\partial \xi} \right)_{\xi=0}, \quad (8.14)$$

$$\frac{\sin \eta}{2(1 - \cos \eta)} \tilde{Q}(\eta, 0) + \tilde{U}_2(\eta, 0) = \epsilon \left(\frac{1}{2} \sin \eta \frac{\partial \tilde{Q}}{\partial \xi} + (1 - \cos \eta) \frac{\partial \tilde{U}_2}{\partial \xi} \right)_{\xi=0}, \quad (8.15)$$

$$\tilde{w}(\eta, 0) = -\epsilon \left(\tilde{Q} - \frac{1}{2} \sin \eta \frac{\partial \tilde{Q}}{\partial \eta} - \frac{1}{2} (1 - \cos \eta) \left(\frac{\partial \tilde{U}_2}{\partial \eta} + \frac{\partial \tilde{U}_0}{\partial \eta} - \frac{2\tilde{U}_2}{\sin \eta} \right) \right)_{\xi=0}. \quad (8.16)$$

Making use of the recursion relations for the Legendre polynomials, three recursion relations for these interfacial constraint conditions can be obtained by substituting the series solutions given by (5.6)–(5.9) into (8.14)–(8.16). The recursion relations derived from these conditions are given in Appendix B.

Finally, substituting (8.9) into (8.7) and (8.8), the significant asymptotic solutions for the velocity components in the Brinkman medium are given to leading order in ϵ by

$$v_r^* \sim \frac{1}{2} V (r \tilde{Q}(r, 0) + \tilde{U}_0(r, 0) + \tilde{U}_2(r, 0)) e^{z/\epsilon} \cos \theta, \quad (8.17)$$

$$v_\theta^* \sim \frac{1}{2} V (\tilde{U}_2(r, 0) - \tilde{U}_0(r, 0)) e^{z/\epsilon} \sin \theta, \quad (8.18)$$

$$v_z^* \sim V \tilde{w}(r, 0) e^{z/\epsilon} \cos \theta. \quad (8.19)$$

Substituting (5.4) into the first of (7.7), the solution for the pressure, which represents an exact solution to Laplace's equation, is given by

$$p^* = \frac{\mu V}{c} \cos \theta \int_0^\infty {}_1\tilde{Q}(s, 0) e^{sz} J_1(sr) s ds, \quad (8.20)$$

where the order- n generalized Hankel transform of the function $\varphi(r)$ is defined as

$${}_n\varphi(s) := \int_0^\infty \varphi(r) J_n(sr) r dr \implies \varphi(r) = \int_0^\infty {}_n\varphi(s) J_n(sr) s ds.$$

Thus, (8.17)–(8.19) asymptotically satisfy the momentum equations in the Brinkman medium, given by (3.1)–(3.3), whereas (8.20) and the series solutions, given by (5.6)–(5.9), exactly satisfy the momentum equations in the Stokes-flow region, given by (4.2), and Laplace's equation for the pressure throughout both the Brinkman and Stokes-flow regions. By further imposing the eight recursion relations, consisting of the two given by (5.10) and (5.11), a set of three given in Appendix A, and the three given by (B 1)–(B 3) in Appendix B, the solution found here exactly satisfies the continuity equations throughout both the Brinkman and Stokes-flow regions, given respectively by (3.9) and (4.3), the no-slip boundary condition on the sphere surface, and the six interfacial velocity and stress-traction conditions given by (7.2)–(7.4).

The assumption advanced earlier about the rate of decay of $A(s)$, $E(s)$, and $G(s)$ can now be verified. Substituting (5.6), (5.8), and (5.9) into (8.9) and using (4.1) to express η in terms of r at $z = \xi = 0$, inverse generalized Hankel transforms can be

performed on the resulting expressions for $C_0(r)$, $C_1(r)$, and $C_2(r)$ to yield the leading-order asymptotic expressions for the functions $A(s)$, $E(s)$, and $G(s)$, which are given in Appendix C. The resulting expressions decay exponentially fast in s . In principle, there will be some characteristic decay frequency, s_c , for the quantities $A(s)$, $E(s)$, and $G(s)$, where each are of the form $\exp(-s/s_c)$. If s_c is smaller than the Gaussian width $2/(\epsilon z)$, then the approximation made earlier (i.e. replacing the Gaussian with a constant) is justified. In particular, this approximation is valid for $\epsilon \ll 2/(s_c z)$, where it can be shown that s_c is of order unity. For a given value of ϵ then, there exists a boundary-layer region where this approximation is reasonable. For larger values of $|z|$ outside the boundary layer, the solution begins to break down. However, since the solution in the Brinkman region decays exponentially in z , the error for large values of $|z|$ will be negligible if ϵ is sufficiently small. Based on numerical results, we estimate that the asymptotic solution presented here is a very good approximation throughout the Brinkman and Stokes-flow regions if $\epsilon \lesssim 0.25$.

9. Drag force on the sphere and torque about the sphere centre

Using the exact series solutions, Dean & O'Neill (1963) and O'Neill (1964) analytically determined the hydrodynamic drag force, $\mathbf{F} = (F_x, F_y, F_z)$, exerted on the sphere and torque, $\mathbf{T} = (T_x, T_y, T_z)$, about the sphere centre, for the cases of pure rotation and pure translation of a sphere in an otherwise quiescent fluid near a plane. If the plane is replaced by a Brinkman half-space, one finds that the series solutions provided by Dean & O'Neill (1963) and O'Neill (1964) for the drag force and torque need a slight modification for \mathbf{T} but no modification for \mathbf{F} . Following the procedure of Dean & O'Neill (1963) and O'Neill (1964), it can be shown that, in the presence of a Brinkman half-space, the exact form of the series solutions for the Cartesian components of \mathbf{F} and \mathbf{T} are given by

$$2^{-1/2} F_x^i = \frac{1}{6} \beta_i \sinh \alpha \sum_{n=1}^{\infty} (n(n+1)d_n + f_{n-1}), \quad F_y = F_z = 0, \quad (9.1)$$

for $i = t, r, s$ where $\beta_t = 1$, $\beta_r = -\sinh \alpha$, and $\beta_s = -\tanh \alpha$, and

$$2^{1/2} T_y^i = \frac{1}{4} \delta_i \sinh^2 \alpha \sum_{n=1}^{\infty} (2n(n+1)(a_n + b_n) - (2n+1)(e_{n-1} + f_{n-1})) \\ + \coth \alpha (n(n+1)(c_n + d_n) + (e_{n-1} + f_{n-1})), \quad T_x = T_z = 0, \quad (9.2)$$

for $i = t, r, s$ where $\delta_t = 1$, $\delta_r = -\sinh \alpha$, and $\delta_s = -2 \sinh \alpha$. In (9.1) and (9.2), the superscripts t , r , and s correspond, respectively, to pure translation, pure rotation, and uniform shear.

10. Free motion of a neutrally buoyant sphere

In the case of a neutrally buoyant sphere in a uniform shear flow, Ω and U cannot be specified independently. In order to obtain the rotational and translational speeds associated with the free motion of a neutrally buoyant sphere in a uniform shear field, the sum of the externally applied viscous drag forces on the sphere, and the sum of the external torques about the centre of the sphere must vanish. Goldman *et al.* (1967*b*) showed that for a neutrally buoyant sphere translating in the x -direction and rotating about the y -axis, these conditions can be satisfied simultaneously for Ω

and U if we require that

$$\frac{\Omega}{\frac{1}{2}\dot{\gamma}} = \frac{2(d/a)F_x^s T_y^t - F_x^t T_y^s}{F_x^t T_y^r - F_x^r T_y^t}, \quad \frac{U}{d\dot{\gamma}} = \frac{\frac{1}{2}(a/d)F_x^r T_y^s - F_x^s T_y^r}{F_x^t T_y^r - F_x^r T_y^t}. \quad (10.1)$$

In (10.1) the dimensionless force and torque components are defined relative to their dimensional counterparts according to

$$F_x^r = \frac{F_x^{*r}}{6\pi\mu\Omega a^2}, \quad F_x^t = \frac{F_x^{*t}}{6\pi\mu U a}, \quad F_x^s = \frac{F_x^{*s}}{6\pi\mu\dot{\gamma} a d},$$

$$T_y^r = \frac{T_y^{*r}}{8\pi\mu\Omega a^3}, \quad T_y^t = \frac{T_y^{*t}}{8\pi\mu U a^2}, \quad T_y^s = \frac{T_y^{*s}}{4\pi\mu\dot{\gamma} a^3}.$$

Thus the free motion of a neutrally buoyant sphere rotating and translating in a uniform shear field near a Brinkman half-space is fully characterized by Ω and U given by (10.1). Determination of these two quantities not only provides the free motion of a neutrally buoyant sphere, but also leads to the appropriate scaling of the dimensionless velocity and pressure fields associated with the three elemental problems we have considered such that linear superposition of the scaled solutions provides the velocity and pressure fields for the neutrally buoyant case as well.

11. Results

The solution for a particular point in the two-dimensional parameter space (α, ϵ) for each of the three cases considered is uniquely determined by the eight sets of coefficients, $\{a_n, b_n, c_n, d_n, e_{n-1}, f_{n-1}, g_{n+1}, h_{n+1}\}$ for $n = 1, 2, \dots$. In order to make this determination, we must first truncate the infinite series solutions for \tilde{Q} , \tilde{w} , \tilde{U}_0 , and \tilde{U}_2 in the Stokes-flow region and retain only the leading N terms in each series. The $8N$ coefficients are then found that uniquely satisfy the $8N$ system of linear equations derived from the $3N$ recursion relations (see Appendix A) obtained from the three no-slip boundary conditions on the sphere surface, the $2N$ recursion relationships given by (5.10) and (5.11) obtained from the continuity equation in the Stokes-flow region, and the $3N$ recursion relationships (see Appendix B) obtained from the three constraint equations given by (8.14)–(8.16).

Since all of the series solutions are convergent, accuracy increased with increasing N . As expected, in order to achieve a given accuracy, a greater number of terms in the series solutions had to be retained for small values of α (corresponding to small clearances between the sphere and the interfacial plane, P) than for large values. However, as N increased, the determinant of the $8N \times 8N$ matrix associated with the $8N$ system of linear equations decreased. Using traditional numerical methods, the number of terms that could be retained in the series solutions was then limited by machine precision since increasing N above a certain threshold resulted in an ill-conditioned matrix as far as the precision of the calculations was concerned. Upon inversion, that resulted in the accumulation of significant numerical errors in the $8N$ coefficients. To obviate this limitation, all calculations were carried out using multiple precision. Furthermore, when assembling the $8N \times 8N$ matrix, all matrix elements were left in symbolic form or as rational fractions whenever possible, with conversion to their floating-point approximations being left as a final step before matrix inversion. When computing the series solutions for all of the results presented here, we set $N = 45$ and carried 50 digits of precision. Using these settings, the boundary conditions on the sphere surface, the continuity equation throughout the Stokes-flow region, and

the interfacial velocity and stress conditions were satisfied with an accuracy that exceeded machine precision. Because of the need for multiple precision calculations and for symbolic manipulation of the $8N$ system of linear equations, all computations were performed using a symbolic algebra package (*Mathematica*, Wolfram Research, Inc.) on Power Macintosh G4-based computers (Apple Computer, Inc.). With $N = 45$, calculations of the $8N$ coefficients carrying 50 digits of precision took approximately 2 orders of magnitude longer than machine precision calculations (~ 2 s with machine precision versus ~ 200 s with 50 digits of precision using a 1.25 GHz G4 processor).

It was noted, not surprisingly, that for a given point in the parameter space (α, ϵ), solutions for the case of uniform shear required retention of a greater number of terms to achieve a given accuracy than did solutions for the cases of pure translation and pure rotation. When calculating the drag force and torque on the sphere, we did not compute the coefficients for the case of uniform shear at each of the points in the parameter space considered since this would have required the retention of many more terms in the series solutions than were necessary in the other two cases if comparable accuracy was to be obtained. Instead, all of the information required to compute drag force and torque for the case of uniform shear is obtainable from the coefficients associated with the other two cases by invoking a quadrature method first conceived by Brenner (1964) and later implemented by Goldman (1966). There it was shown, through consideration of the stress-traction vector on the sphere surface, that for the case of uniform shear, the drag force on the sphere and the torque about the sphere centre could be determined from the coefficients of the pure translational and pure rotational problems, respectively. The same arguments apply to this problem, where the sphere is in proximity to a Brinkman half-space.

Figure 2 shows the magnitudes of the dimensionless drag force (black curves, left axis) and torque about the sphere centre (grey curves, right axis), on a purely translating sphere (*a*), a purely rotating sphere (*b*), and a stationary sphere in a uniform shear field (*c*) of radius a near a Brinkman half-space for various values of dimensionless permeability, $\epsilon_a^2 = (c/a)^2 \epsilon^2$, as a function of the dimensionless distance, d/a , between the interface, P , and the sphere centre. Figure 3 shows the relative translational (*a*) and rotational (*b*) speeds for the free motion of a neutrally buoyant sphere near a Brinkman half-space in a uniform shear field, with the constant shear rate $\dot{\gamma}$, as a function of d/a for various values of ϵ_a^2 . (Since c varies with d/a , so too does the dimensionless permeability, ϵ^2 , if μ and K are constant. Therefore, ϵ^2 varies for constant values of μ , K , and a along all but the solid curves shown in figures 2 and 3. It is often more convenient, therefore, to show results in terms of ϵ_a^2 , the dimensionless permeability based on sphere radius, a .) The dashed line in figures 3(*a*) and 3(*b*) corresponds to one extreme of a sphere in an unbounded Newtonian fluid (i.e. as $K \rightarrow 0$, $\epsilon_a^2 \rightarrow \infty$) whereas the solid curve in each panel of figures 2 and 3 corresponds to the other extreme in which there is no flow through the layer (i.e. as $K \rightarrow \infty$, $\epsilon_a^2 \rightarrow 0$). In each case, these represent upper and lower bounds on the magnitudes of the associated quantities being plotted, while the three intermediate curves represent dimensionless permeabilities of the Brinkman medium corresponding to $\epsilon_a^2 = 1.92 \times 10^{-1}$, 1.92×10^{-2} , and 1.92×10^{-3} . These three values correspond to dimensional hydraulic resistivity values of $K = 10^8$, 10^9 , and 10^{10} dyn s cm $^{-4}$, respectively, for a viscosity $\mu = 0.012$ dyn s cm $^{-2}$ and a sphere radius $a = 0.25$ μ m. These particular dimensional parameters are relevant to a recent study (Smith *et al.* 2003) of systemically injected, neutrally buoyant, fluorescent microspheres circulating in the plasma-rich region near the vessel wall of post-capillary venules *in vivo* (see § 12). In figures 2 and 3, the range of d/a shown corresponds to $\ln(3/2) \leq \alpha \leq \ln 10$

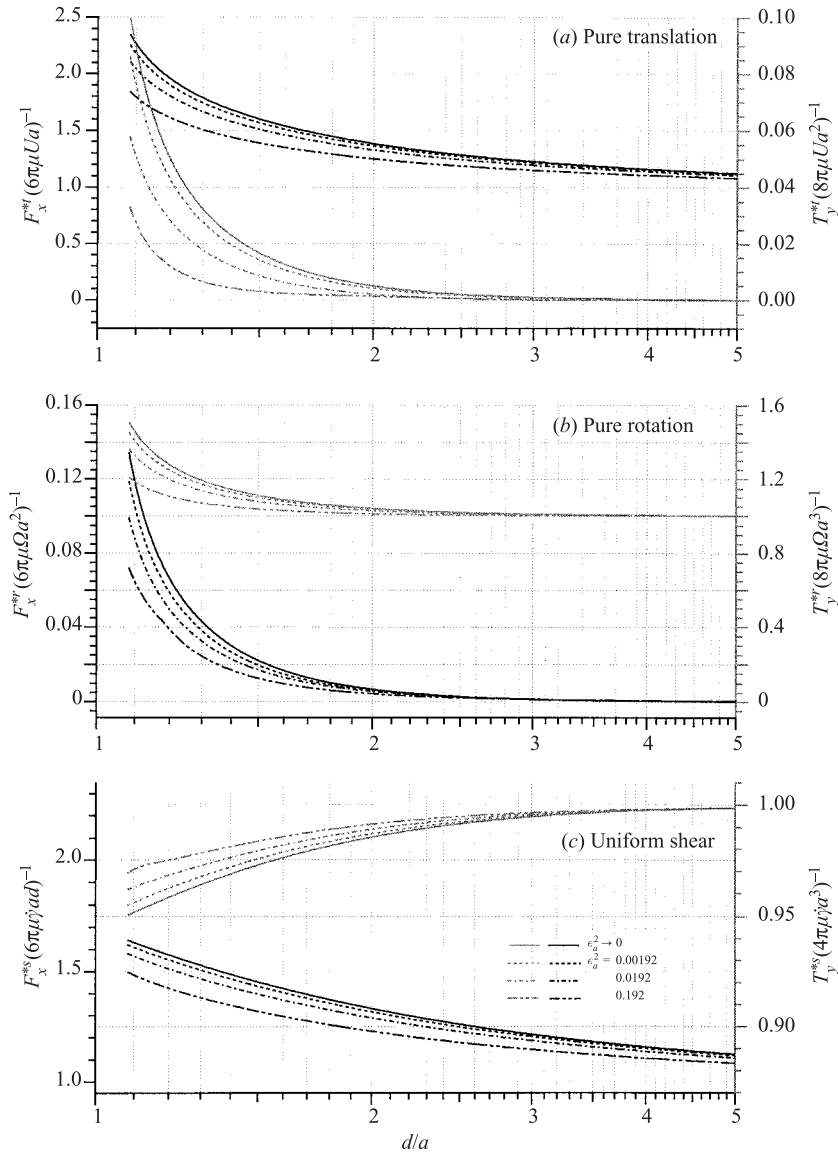


FIGURE 2. Variation, with respect to d/a , of the magnitudes of the dimensionless drag force on a sphere (black curves, left axis) and torque on a sphere about its centre (grey curves, right axis) if the sphere, having radius a and centred a distance d above a Brinkman half-space, is (a) translating without rotation through an otherwise quiescent fluid, or (b) rotating without translation in an otherwise quiescent fluid, or (c) fixed in a uniform shear field. All cases are shown for the same three values of the dimensionless permeability, ϵ_a^2 , and for a vanishing permeability (solid curves) when the Brinkman medium is replaced by a plane of infinite extent.

($0.41 \lesssim \alpha \lesssim 2.3$). This range corresponds to a dimensionless minimal clearance between the sphere and the interfacial plane, P , of $0.08 \lesssim (d/a) - 1 \lesssim 4.05$, which, in terms of the dimensional parameters referenced above, corresponds to a minimal clearance range of $0.02 \lesssim d - a \lesssim 1.01 \mu\text{m}$.

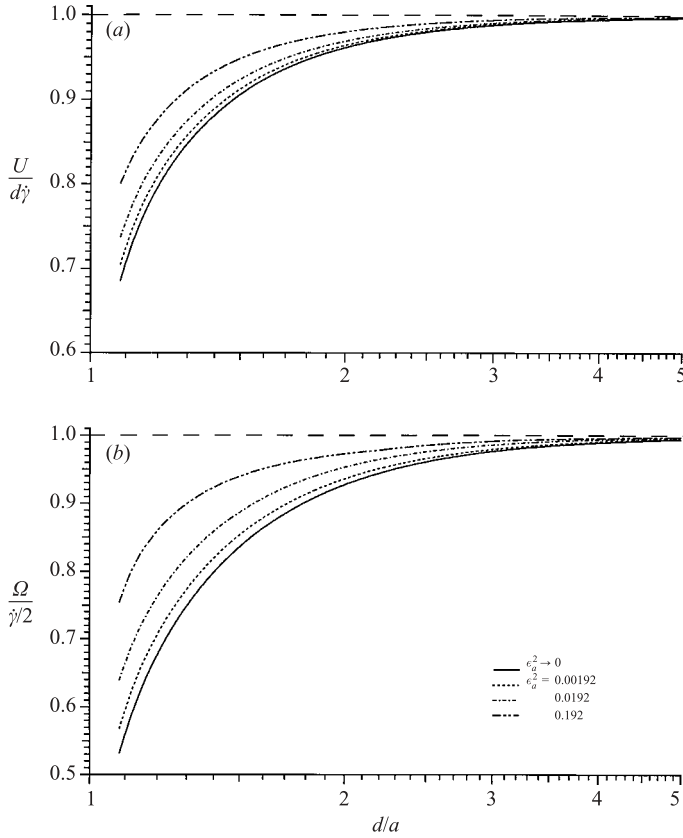


FIGURE 3. Variation, with respect to d/a , of the relative (a) translational speed, $U/(d\dot{\gamma})$, and (b) rotational speed, $2\Omega/\dot{\gamma}$, for the free motion of a neutrally buoyant sphere, of radius a , in a uniform shear field centred a distance d above a Brinkman half-space, for the same three values of ϵ_a^2 shown in figure 2. The curves in (a) represent the transformation between the translational speed of a sphere centred a distance d above the interface and the translational speed, $d\dot{\gamma}$, a fluid particle would have, located a distance d above the interface, in a uniform shear field in the absence of the sphere. The curves in (b) represent the transformation between the rotational speed of that sphere and the constant solid-body rotation, $\dot{\gamma}/2$, a fluid particle would have in a uniform shear field in the absence of the sphere.

Figure 4 shows the dimensionless radial velocity profiles in the (x, z) -plane at $y=0$ under the ‘south pole’ of a purely translating sphere (a), a purely rotating sphere (b), a stationary sphere in a uniform shear flow (c), and a neutrally buoyant sphere in a uniform shear flow (d) near a Brinkman half-space, as a function of the dimensionless distance, z^*/a , below the sphere for the same three non-vanishing values of ϵ_a^2 shown in figures 2 and 3. The interfacial plane, P , between the Brinkman (shaded) and Stokes-flow (unshaded) regions is located at $z=0$. Figure 5 shows the dimensionless pressure distribution, Q , in the (x, z) -plane at $y=0$ along the interfacial plane, P , and at four equally spaced depths below P arising from a Stokes flow generated by the motion of a neutrally buoyant sphere in a uniform shear field above a Brinkman half-space having a dimensionless permeability corresponding to $\epsilon_a^2 = 1.92 \times 10^{-3}$. All calculations in figures 4 and 5 were performed for a minimal clearance of $\sim 1.032a$ ($\alpha = \ln(3.8) \approx 1.335$).

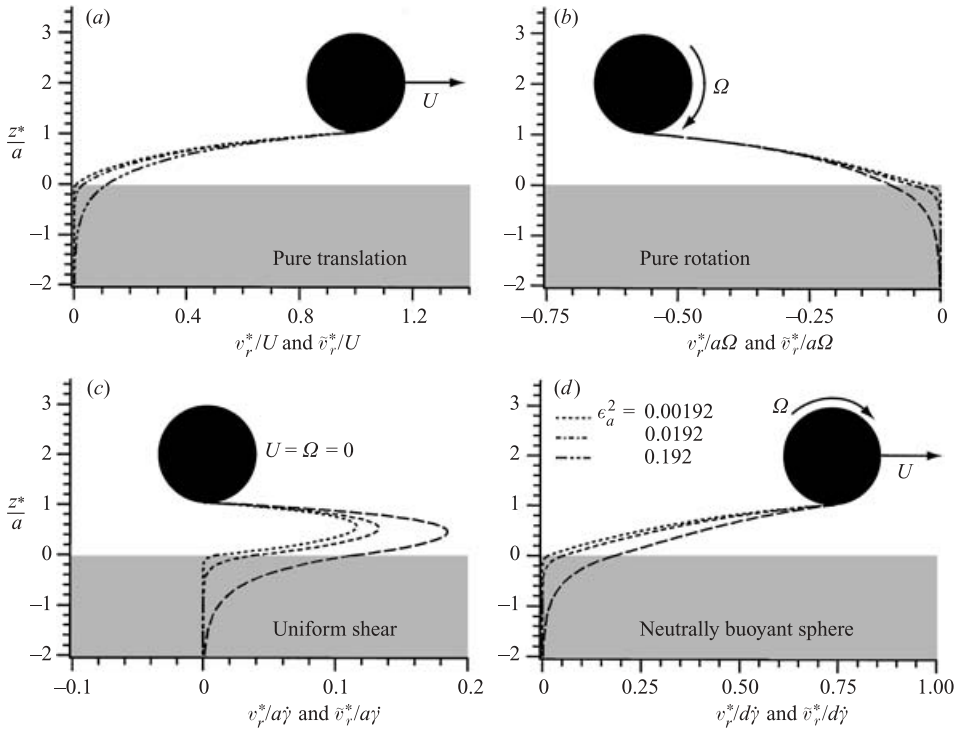


FIGURE 4. Dimensionless radial velocity profiles under the south pole of (a) a purely translating sphere, (b) a purely rotating sphere, (c) a stationary sphere in a uniform shear flow, and (d) a neutrally buoyant sphere in free motion in a uniform shear field near a Brinkman half-space for the same three non-zero values of ϵ_a^2 shown in figure 2. Note, abscissa ranges vary.

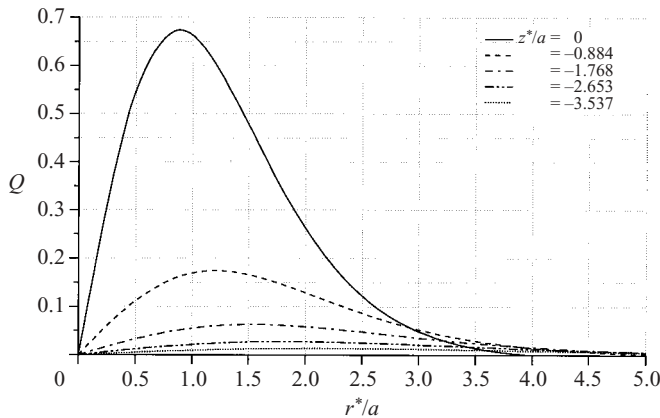


FIGURE 5. Dimensionless pressure variations at $y=0$ along the interfacial plane, P (solid curve), and along four equally spaced (x,y) -planes below P arising from a Stokes flow generated by the free motion of a neutrally buoyant sphere in a uniform shear field above a Brinkman half-space. The dimensionless permeability corresponds to $\epsilon_a^2 = 1.92 \times 10^{-3}$ and the minimal clearance between the sphere and the interfacial plane is as in figure 4.

12. Application to near-wall microfluidics in post-capillary venules

A major motivation for this work has been to determine the influence of a nearby porous permeable medium on the free motion of a neutrally buoyant sphere in a Stokes flow. Having made this determination, measurements of sphere motion in the vicinity of a porous medium could provide a means for characterizing properties of that medium. A particular application of these results is to use such measurements to probe the extent to which the glycocalyx surface layer, expressed on the vascular endothelium of microvessels, extends into the vessel lumen and the effect it has on near-wall microfluidics.

The glycocalyx is an endothelial-cell surface layer consisting of membrane-bound macromolecules that include proteoglycans, glycoproteins, glycosaminoglycans, and perhaps adsorbed plasma proteins from the blood. The first successful attempt at visualizing the layer *in vivo* was achieved through the identification of a near-wall steric exclusion zone of fluorescently labelled macromolecular plasma tracers (Vink & Duling 1996). In capillaries and small post-capillary venules, Duling and coworkers have shown that 70 kDa FITC-dextran was excluded from a region $\sim 0.4\text{--}0.5\ \mu\text{m}$ in thickness adjacent to the endothelial-cell surface (Vink & Duling 1996; Henry & Duling 1999). This dye-exclusion technique, however, has not been conclusive in vessels larger than $\sim 12\text{--}15\ \mu\text{m}$ in diameter because of problems associated with light refraction of the fluorescent dye column near the vessel wall (Henry & Duling 1999). An alternative approach for investigating the layer *in vivo* has recently been developed by Smith *et al.* (2003), who used near-wall fluorescent intravital micro-particle image velocimetry (μ -PIV) to image $\sim 500\ \text{nm}$ neutrally buoyant fluorescent polystyrene microspheres circulating in the plasma-rich zone of post-capillary venules in the mouse cremaster muscle. Not only were they able to obtain an estimate of layer thickness with this approach (ranging between ~ 0.33 and $0.44\ \mu\text{m}$), which was comparable to the estimate derived from the dye exclusion technique, but their μ -PIV data also provided the first direct evidence for a hydrodynamically relevant glycocalyx surface layer in venules *in vivo*.

Based on the analysis presented here, Smith *et al.* (2003) inferred fluid-particle speeds near the vessel wall from measured microsphere translational speeds using the second of (10.1) (see figure 3*a*). Starting with an initial guess of layer thickness, a linear regression through the predicted fluid-particle speeds was then used, together with the analysis of Damiano *et al.* (1996), to converge upon estimates of layer thickness over a range of possible values of hydraulic resistivity, K . The applicability of the analysis presented here to near-wall microfluidics in venules depends on the validity of certain assumptions.

First, microspheres must be sufficiently small, and the vessel diameter sufficiently large, such that the curvature of the vessel wall can be neglected and the flow just outside the glycocalyx can be regarded, in the absence of microspheres, as a uniform shear field. For $500\ \text{nm}$ microspheres in $25\text{--}40\ \mu\text{m}$ -diameter venules, both of these approximations are very accurate. The uniform-shear approximation, in particular, is reasonable since red cells tend to shun the wall in microvessels, leading to a plasma-rich region, of ~ 2 to $3\ \mu\text{m}$ in thickness, near the vessel wall.

Second, a uniform Brinkman medium making a discrete interface with a homogeneous viscous fluid must be representative, in a mean sense, of a glycocalyx that varies axially in thickness and axially and radially in hydraulic resistivity, K . If these quantities are represented by their mean values, then this idealization is nevertheless quantitatively useful since it follows, from the mean-value theorem for

integrals of continuous functions, that these quantities are bounded by the largest and smallest values they would assume in a heterogeneous spatially non-uniform glycocalyx. Furthermore, invoking a Brinkman medium (rather than a more general description using something like mixture theory) as a first approximation of the glycocalyx surface layer is likely to be reasonable when one considers the very low solid-volume fractions the layer is thought to have (Damiano *et al.* 1996; Feng & Weinbaum 2000). It is not uncommon for mucopolysaccharide structures devoid of collagen to contain solid-volume fractions less than 1%. In such a case, the viscosity of the fluid constituent within these structures is very nearly equal to that of the external fluid. We therefore assume that the viscosity, μ , of the fluid in the Brinkman-medium model is simply equal to that of the surrounding blood plasma. Even with very low solid-volume fractions, the hydraulic resistivity, K , of the layer can nevertheless be large enough to render the Darcy drag an important determinant of the flow (Damiano *et al.* 1996). Recent analytical studies have attempted to put bounds on K . Using an estimate of glycocalyx fixed-charge density, based on an electrochemical model of the glycocalyx (Stace & Damiano 2001), Damiano & Stace (2002) were able to estimate the hydraulic resistivity of the glycocalyx from their mechano-electrochemical model of the layer to be between 10^{10} and 10^{11} dyn s cm⁻⁴. This is consistent with an earlier estimate by Feng & Weinbaum (2000), which was inferred from a fibre matrix model of the glycocalyx based on the Brinkman equation.

Finally, for the asymptotic approximation invoked here to be valid, we require that $\epsilon_a \ll 1$. This condition is certainly met for the values of K , μ , and a referenced above and is reasonably well satisfied for values of K as small as 10^8 dyn s cm⁻⁴. The fact that the layer itself is of finite thickness, t , whereas the analysis developed here assumes a Brinkman half-space, does not pose a problem so long as the predicted fluid velocity in the half-space decays sufficiently fast so as to nearly satisfy the no-slip condition at the vessel wall. In particular, if $|\epsilon_a \ln(0.01)| \lesssim t/a$, then the fluid velocity at $z^* = -t$ will be less than $\sim 1\%$ of the slip velocity on the interfacial plane, P . For material and geometric properties thought to be typical of the glycocalyx (Damiano *et al.* 1996; Damiano & Stace 2002; Feng & Weinbaum 2000; Smith *et al.* 2003), and prevailing flow conditions typical of the microcirculation, this condition is also met (e.g. see figure 4d for values of $K \gtrsim 10^8$ dyn s cm⁻⁴ assuming a glycocalyx thickness and microsphere diameter of ~ 0.5 μ m).

Partial support for this work was contributed by the Whitaker Foundation, RG-98-0524, and the National Science Foundation, BES-0093985.

Appendix A. Recursion relations for the no-slip boundary conditions on the sphere, S

A.1. Pure translation

Substituting the series solutions given by (5.6)–(5.9) into (6.4), and using the recursion relations for the Legendre polynomials, it can be shown that the no-slip boundary condition on the sphere surface for the case of pure translation is satisfied if

$$\begin{aligned} & \frac{\kappa_n - \coth \alpha}{2n - 1} (f_{n-1} + (n - 2)(n - 1) h_{n-1}) + \frac{\kappa_n + \coth \alpha}{2n + 3} (f_{n+1} + (n + 2)(n + 3) h_{n+1}) \\ & - \frac{\lambda_n - 1}{2n - 1} (e_{n-1} + (n - 2)(n - 1) g_{n-1}) + \frac{\lambda_n + 1}{2n + 3} (e_{n+1} + (n + 2)(n + 3) g_{n+1}) \\ & = 4 \mu_n, \quad n = 1, 2, \dots, \quad (\text{A } 1) \end{aligned}$$

$$\begin{aligned} & \frac{\kappa_n - \coth \alpha}{2n-1} (d_{n-1} - 2(n-2)h_{n-1}) + \frac{\kappa_n + \coth \alpha}{2n+3} (d_{n+1} + 2(n+3)h_{n+1}) \\ & - \frac{\lambda_n - 1}{2n-1} (c_{n-1} - 2(n-2)g_{n-1}) + \frac{\lambda_n + 1}{2n+3} (c_{n+1} + 2(n+3)g_{n+1}) \\ & = 2 \coth \alpha (\kappa_n g_n + h_n), \quad n = 2, 3, \dots, \end{aligned} \quad (\text{A } 2)$$

$$\begin{aligned} & \frac{\lambda_n - 1}{2n-1} a_{n-1} - \frac{\lambda_n + 1}{2n+3} a_{n+1} - \frac{\kappa_n - \coth \alpha}{2n-1} b_{n-1} - \frac{\kappa_n + \coth \alpha}{2n+3} b_{n+1} \\ & = \kappa_n g_n + h_n, \quad n = 2, 3, \dots, \end{aligned} \quad (\text{A } 3)$$

where $\kappa_n = \coth(n + \frac{1}{2})\alpha$, $\lambda_n = \kappa_n \coth \alpha$, and

$$\mu_n = \frac{2^{-1/2}}{\sinh \alpha \sinh (n + \frac{1}{2})\alpha} \left(\frac{e^{-(n+3/2)\alpha}}{2n+3} - \frac{e^{-(n-1/2)\alpha}}{2n-1} \right).$$

In (A 1), we made use of the series expansion

$$(\cosh \alpha - \cos \eta)^{-1/2} = - \sum_{n=1}^{\infty} 2 \mu_n \sinh \alpha \sinh (n + \frac{1}{2})\alpha P'_n(\cos \eta). \quad (\text{A } 4)$$

A.2. Pure rotation

Substituting (5.6)–(5.9) into (6.9) and (6.10), and using the recursion relations for the Legendre polynomials, it can be shown that the no-slip boundary condition on the sphere surface for the case of pure rotation is satisfied if

$$\begin{aligned} & \frac{\kappa_n - \coth \alpha}{2n-1} (f_{n-1} + (n-2)(n-1)h_{n-1}) + \frac{\kappa_n + \coth \alpha}{2n+3} (f_{n+1} + (n+2)(n+3)h_{n+1}) \\ & - \frac{\lambda_n - 1}{2n-1} (e_{n-1} + (n-2)(n-1)g_{n-1}) + \frac{\lambda_n + 1}{2n+3} (e_{n+1} + (n+2)(n+3)g_{n+1}) \\ & = -4 \coth \alpha \mu_n + 2^{3/2} \left(\frac{e^{-(n+3/2)\alpha} - e^{-(n-1/2)\alpha}}{\sinh \alpha \sinh (n + \frac{1}{2})\alpha} \right), \quad n = 1, 2, \dots, \end{aligned} \quad (\text{A } 5)$$

$$\begin{aligned} & \frac{\kappa_n - \coth \alpha}{2n-1} (d_{n-1} - 2(n-2)h_{n-1}) + \frac{\kappa_n + \coth \alpha}{2n+3} (d_{n+1} + 2(n+3)h_{n+1}) \\ & - \frac{\lambda_n - 1}{2n-1} (c_{n-1} - 2(n-2)g_{n-1}) + \frac{\lambda_n + 1}{2n+3} (c_{n+1} + 2(n+3)g_{n+1}) \\ & = 2 \coth \alpha (\kappa_n g_n + h_n), \quad n = 2, 3, \dots, \end{aligned} \quad (\text{A } 6)$$

$$\begin{aligned} & \frac{\lambda_n - 1}{2n-1} a_{n-1} - \frac{\lambda_n + 1}{2n+3} a_{n+1} - \frac{\kappa_n - \coth \alpha}{2n-1} b_{n-1} - \frac{\kappa_n + \coth \alpha}{2n+3} b_{n+1} \\ & = \kappa_n g_n + h_n + 4 \mu_n, \quad n = 2, 3, \dots \end{aligned} \quad (\text{A } 7)$$

In (A 5) and (A 7), we made use of the series expansions

$$\sinh \alpha (\cosh \alpha - \cos \eta)^{-3/2} = \sum_{n=0}^{\infty} 2^{1/2} (2n+1) e^{-(n+1/2)\alpha} P_n(\cos \eta), \quad (\text{A } 8)$$

$$(\cosh \alpha - \cos \eta)^{-3/2} = - \sum_{n=2}^{\infty} 4 \mu_n \sinh \alpha \sinh (n + \frac{1}{2})\alpha P''_n(\cos \eta). \quad (\text{A } 9)$$

A.3. Uniform shear

Substituting (5.6)–(5.9) into (6.12) and (6.13), and using the recursion relations for the Legendre polynomials, it can be shown that the no-slip boundary condition on the surface of a stationary sphere in a uniform shear field is satisfied if

$$\begin{aligned} & \frac{\kappa_n - \coth \alpha}{2n-1} (f_{n-1} + (n-2)(n-1)h_{n-1}) + \frac{\kappa_n + \coth \alpha}{2n+3} (f_{n+1} + (n+2)(n+3)h_{n+1}) \\ & - \frac{\lambda_n - 1}{2n-1} (e_{n-1} + (n-2)(n-1)g_{n-1}) + \frac{\lambda_n + 1}{2n+3} (e_{n+1} + (n+2)(n+3)g_{n+1}) \\ & = -4\epsilon \mu_n - 2^{3/2} \left(\frac{e^{-(n+3/2)\alpha} - e^{-(n-1/2)\alpha}}{\sinh \alpha \sinh(n + \frac{1}{2})\alpha} \right), \quad n = 1, 2, \dots, \quad (\text{A } 10) \end{aligned}$$

$$\begin{aligned} & \frac{\kappa_n - \coth \alpha}{2n-1} (d_{n-1} - 2(n-2)h_{n-1}) + \frac{\kappa_n + \coth \alpha}{2n+3} (d_{n+1} + 2(n+3)h_{n+1}) \\ & - \frac{\lambda_n - 1}{2n-1} (c_{n-1} - 2(n-2)g_{n-1}) + \frac{\lambda_n + 1}{2n+3} (c_{n+1} + 2(n+3)g_{n+1}) \\ & = 2 \coth \alpha (\kappa_n g_n + h_n), \quad n = 2, 3, \dots, \quad (\text{A } 11) \end{aligned}$$

$$\begin{aligned} & \frac{\lambda_n - 1}{2n-1} a_{n-1} - \frac{\lambda_n + 1}{2n+3} a_{n+1} - \frac{\kappa_n - \coth \alpha}{2n-1} b_{n-1} - \frac{\kappa_n + \coth \alpha}{2n+3} b_{n+1} \\ & = \kappa_n g_n + h_n, \quad n = 2, 3, \dots \quad (\text{A } 12) \end{aligned}$$

In (A 10), we made use of the series expansions given by (A 4) and (A 8).

Appendix B. Recursion relations for the interfacial conditions on the plane, P

Substituting (5.6)–(5.9) into (8.14)–(8.16), and using the recursion relations for the Legendre polynomials, it can be shown that the three interfacial constraints are satisfied if

$$\begin{aligned} & -\frac{(n-1)(n-2)c_{n-2}}{2(2n-1)(2n-3)} + \frac{n(n+1)c_n}{(2n+3)(2n-1)} - \frac{(n+3)(n+2)c_{n+2}}{2(2n+5)(2n+3)} - \frac{(n-1)e_{n-2}}{(2n-1)(2n-3)} \\ & + \frac{e_{n-1}}{2n-1} - \frac{e_n}{(2n+3)(2n-1)} - \frac{e_{n+1}}{2n+3} + \frac{(n+2)e_{n+2}}{(2n+5)(2n+3)} \\ & + \epsilon \left(-\frac{(n-1)(n-2)(n-3)d_{n-3}}{4(2n-1)(2n-3)} + \frac{(n-1)(n-2)d_{n-2}}{4(2n-1)} + \frac{n^2(n-1)d_{n-1}}{4(2n+3)(2n-3)} \right. \\ & - \frac{n(2n+1)(n+1)d_n}{2(2n+3)(2n-1)} + \frac{(n+1)^2(n+2)d_{n+1}}{4(2n+5)(2n-1)} + \frac{(n+3)(n+2)d_{n+2}}{4(2n+3)} \\ & - \frac{(n+4)(n+3)(n+2)d_{n+3}}{4(2n+5)(2n+3)} - \frac{(n-1)(n-2)f_{n-3}}{2(2n-1)(2n-3)} + \frac{(n-1)f_{n-2}}{2n-1} - \frac{(5n^2+n-12)f_{n-1}}{2(2n+3)(2n-3)} \\ & \left. + \frac{(2n+1)f_n}{(2n+3)(2n-1)} + \frac{(5n^2+9n-8)f_{n+1}}{2(2n+5)(2n-1)} - \frac{(n+2)f_{n+2}}{2n+3} + \frac{(n+3)(n+2)f_{n+3}}{2(2n+5)(2n+3)} \right) = 0, \\ & n = 1, 2, \dots, \quad (\text{B } 1) \end{aligned}$$

$$\begin{aligned}
& \frac{c_{n-1}}{4n-2} - \frac{c_{n+1}}{4n+6} - \frac{n-2}{2n-1} g_{n-1} - \frac{n+3}{2n+3} g_{n+1} + \epsilon \left(\frac{n-2}{4(2n-1)} d_{n-2} - \frac{1}{4} d_{n-1} \right. \\
& + \frac{3(2n+1)}{4(2n+3)(2n-1)} d_n + \frac{1}{4} d_{n+1} - \frac{(n+3)}{4(2n+3)} d_{n+2} - \frac{(n-2)(n-3)}{2(2n-1)} h_{n-2} + (n-2) h_{n-1} \\
& \left. - \frac{3(2n+1)(n+2)(n-1)}{(2n+3)(2n-1)} h_n + (n-2) h_{n+1} - \frac{(n+4)(n+3)}{2(2n+3)} h_{n+2} \right) = 0, \\
& n = 2, 3, \dots, \quad (\text{B } 2)
\end{aligned}$$

$$\begin{aligned}
& \frac{-(n-2)a_{n-2}}{(2n-1)(2n-3)} + \frac{a_{n-1}}{2n-1} - \frac{3a_n}{(2n-1)(2n+3)} - \frac{a_{n+1}}{2n+3} + \frac{(n+3)a_{n+2}}{(2n+3)(2n+5)} \\
& + \epsilon \left(\frac{(n-2)(n-3)c_{n-3}}{4(2n-1)(2n-3)} - \frac{n(n-2)c_{n-2}}{2(2n-1)(2n-3)} \right. \\
& - \frac{(2n^3-19n^2+9n+18)c_{n-1}}{4(2n+3)(2n-1)(2n-3)} + \frac{(2n^2+2n-3)c_n}{2(2n+3)(2n-1)} - \frac{(2n^3+25n^2+53n+12)c_{n+1}}{4(2n+5)(2n+3)(2n-1)} \\
& - \frac{(n+3)(n+1)c_{n+2}}{2(2n+5)(2n+3)} + \frac{(n+4)(n+3)c_{n+3}}{4(2n+5)(2n+3)} + \frac{(n-2)e_{n-3}}{4(2n-1)(2n-3)} + \frac{(4n-7)e_{n-2}}{4(2n-1)(2n-3)} \\
& + \frac{(10n^2+5n-33)e_{n-1}}{4(2n+3)(2n-1)(2n-3)} - \frac{5e_n}{2(2n+3)(2n-1)} - \frac{(10n^2+15n-28)e_{n+1}}{4(2n+5)(2n+3)(2n-1)} \\
& + \frac{(4n+11)e_{n+2}}{4(2n+5)(2n+3)} - \frac{(n+3)e_{n+3}}{4(2n+5)(2n+3)} - \frac{(n-2)(n-3)(n-4)g_{n-3}}{4(2n-1)(2n-3)} \\
& + \frac{(4n-3)(n-2)(n-3)g_{n-2}}{4(2n-1)(2n-3)} - \frac{(n-2)(10n^3+19n^2-30n-9)g_{n-1}}{4(2n+3)(2n-1)(2n-3)} + \frac{3(3n^2+3n-1)g_n}{2(2n+3)(2n-1)} \\
& + \frac{(n+3)(10n^3+11n^2-38n-30)g_{n+1}}{4(2n+5)(2n+3)(2n-1)} - \frac{(4n+7)(n+4)(n+3)g_{n+2}}{4(2n+5)(2n+3)} \\
& \left. + \frac{(n+5)(n+4)(n+3)g_{n+3}}{4(2n+5)(2n+3)} \right) = 0, \quad n = 2, 3, \dots \quad (\text{B } 3)
\end{aligned}$$

Appendix C. Asymptotic approximations of $A(s)$, $E(s)$, and $G(s)$

In order to ensure the accuracy of the approximations made in (8.4) and (8.5), it is necessary to establish that the functions $A(s)$, $E(s)$, and $G(s)$ decay rapidly enough over the width of the Gaussian factor, $\exp(\epsilon s^2 z/2)$, such that the Gaussian term and all higher-order terms in ϵ within the integrals of (8.1)–(8.3) can be replaced with unity to good approximation. As described earlier, inverse generalized Hankel transforms can be performed on the expressions for $C_0(r)$, $C_1(r)$, and $C_2(r)$ to yield the leading-order asymptotic expressions for the functions $A(s)$, $E(s)$, and $G(s)$ given by

$$\begin{aligned}
A(s) & \sim \int_0^\infty \epsilon C_1(r) J_1(sr) r dr \\
& = \sum_{n=1}^\infty \sum_{j=1}^n \sum_{k=1}^{j+1} 2(2)^{1/2} j \alpha_{j-1,k}^w P_{j,n} a_n H_1^{1,k+1/2}(s) \\
& = 2(2)^{1/2} e^{-s} (a_1 + (3-2s)a_2 + 2(3-4s+s^2)a_3 + \dots),
\end{aligned}$$

$$\begin{aligned}
 E(s) &\sim \int_0^\infty C_0(r) J_0(sr) r \, dr \\
 &= \sum_{n=1}^\infty \sum_{j=1}^n \sum_{k=1}^{j+1} (2)^{1/2} j \alpha_{j,k}^+ P_{j,n} c_n H_0^{0,k-1/2}(s) + \sum_{n=0}^\infty \sum_{j=0}^n \sum_{k=0}^j (2)^{1/2} \alpha_{j,k}^- P_{j,n} e_n H_0^{0,k+1/2}(s) \\
 &= \frac{(2)^{1/2} e^{-s}}{s} ((1-s)c_1 + (3-7s+2s^2)c_2 + 2(3-11s+7s^2-s^3)c_3 + \dots) \\
 &\quad + \frac{(2)^{1/2} e^{-s}}{s} (e_0 + (1-2s)e_1 + (1-4s+2s^2)e_2 + \dots),
 \end{aligned}$$

$$\begin{aligned}
 G(s) &\sim \int_0^\infty C_2(r) J_2(sr) r \, dr \\
 &= \sum_{n=1}^\infty \sum_{j=1}^n \sum_{k=1}^{j+1} (2)^{1/2} j \alpha_{j,k}^+ P_{j,n} c_n H_2^{0,k-1/2}(s) \\
 &\quad + \sum_{n=2}^\infty \sum_{j=2}^n \sum_{k=1}^{j+1} 4(2)^{1/2} j(j-1) \alpha_{j-1,k}^+ P_{j,n} g_n H_2^{0,k+1/2}(s) \\
 &= \frac{(2)^{1/2} e^{-s}}{s} ((1+s)c_1 + (3+3s-2s^2)c_2 + 2(3+3s-5s^2+s^3)c_3 + \dots) \\
 &\quad + 4(2)^{1/2} s e^{-s} (g_2 + (5-2s)g_3 + (15-12s+2s^2)g_4 + \dots),
 \end{aligned}$$

where

$$H_a^{b,c}(s) = \int_0^\infty \frac{r^b}{(1+r^2)^c} J_a(rs) r \, dr,$$

$P_{n-2k,n} = \frac{(-1)^k}{2^n} \binom{n}{k} \binom{2n-2k}{n}$ is the $(n-2k)$ th coefficient to the n th Legendre polynomial, and

$$\alpha_{j,k}^+ = \begin{cases} \alpha_{j-1,k}^+ - 2\alpha_{j-1,k-1}^+ & \text{for } k \leq j+1 \\ 1 & \text{for } k=1 \\ -1 & \text{for } k=2, j=1 \\ 0 & \text{otherwise,} \end{cases}$$

$$\alpha_{j,k}^- = \begin{cases} \alpha_{j-1,k}^- - 2\alpha_{j-1,k-1}^- & \text{for } k \leq j+1 \\ 1 & \text{for } k=0 \\ -2 & \text{for } k=1, j=1 \\ 0 & \text{otherwise,} \end{cases}$$

$$\alpha_{j,k}^w = \begin{cases} \alpha_{j-1,k}^w - 2\alpha_{j-1,k-1}^w & \text{for } k \leq j+1 \\ 1 & \text{for } k=1 \\ -2 & \text{for } k=2, j=1 \\ 0 & \text{otherwise.} \end{cases}$$

REFERENCES

BEAVERS, G. S. & JOSEPH, D. D. 1967 Boundary conditions at a naturally permeable wall. *J. Fluid Mech.* **30**, 197–207.

- BRENNER, H. 1964 The Stokes resistance to an arbitrary particle – IV Arbitrary fields of flow. *Chem. Engng Sci.* **19**, 703.
- BRINKMAN, H. C. 1947 A calculation of the viscous force exerted by a flowing fluid on a dense swarm of particles. *Appl. Sci. Res. A* **1**, 27–34.
- BRODAY, D. M. 2002 Motion of nanobeads proximate to plasma membranes during single particle tracking. *Bull. Math. Biol.* **64**, 531–563.
- DAMIANO, E. R., DULING, B. R., LEY, K. & SKALAK, T. C. 1996 Axisymmetric pressure-driven flow of rigid pellets through a cylindrical tube lined with a deformable porous wall layer. *J. Fluid Mech.* **314**, 163–189.
- DAMIANO, E. R. & STACE, T. M. 2002 A mechano-electrochemical model of radial deformation of the capillary glycocalyx. *Biophys. J.* **82**, 1153–1175.
- DAVIS, R. H. & STONE, H. A. 1993 Flow through beds of porous particles. *Chem. Engng Sci.* **48**, 3993–4005.
- DEAN, W. R. & O'NEILL, M. E. 1963 A slow motion of viscous liquid caused by the rotation of a solid sphere. *Mathematika* **10**, 13–24.
- FENG, J., GANATOS, P. & WEINBAUM, S. 1998a The general motion of a circular disk in a Brinkman medium. *Phys. Fluids* **10**, 2137–2146.
- FENG, J., GANATOS, P. & WEINBAUM, S. 1998b Motion of a sphere near planar confining boundaries in a Brinkman medium. *J. Fluid Mech.* **375**, 265–296.
- FENG, J. & WEINBAUM, S. 2000 Lubrication theory in highly compressible porous media: the mechanics of skiing, from red cells to humans. *J. Fluid Mech.* **422**, 281–317.
- GOLDMAN, A. J. 1966 Investigations in low Reynolds number fluid–particle dynamics. PhD Thesis, New York University.
- GOLDMAN, A. J., COX, R. G. & BRENNER, H. 1967a Slow viscous motion of a sphere parallel to a plane wall—I Motion through a quiescent fluid. *Chem. Engng Sci.* **22**, 637–651.
- GOLDMAN, A. J., COX, R. G. & BRENNER, H. 1967b Slow viscous motion of a sphere parallel to a plane wall—II Couette flow. *Chem. Engng Sci.* **22**, 653–660.
- GOREN, S. L. & O'NEILL, M. E. 1971 On the hydrodynamic resistance to a particle of a dilute suspension when in the neighbourhood of a large obstacle. *Chem. Engng Sci.* **26**, 325–338.
- HENRY, C. B. S. & DULING, B. R. 1999 Permeation of the luminal capillary glycocalyx is determined by hyaluronan. *Am. J. Physiol.* **277**, H508–H514.
- HOU, J. S., HOLMES, M. H., LAI, W. M. & MOW, V. C. 1989 Boundary conditions at the cartilage-synovial fluid interface for joint lubrication and theoretical verifications. *J. Biomech. Engng* **111**, 78–87.
- HOWELLS, I. D. 1974 Drag due to the motion of a Newtonian fluid through a sparse random array of small fixed rigid objects. *J. Fluid Mech.* **64**, 449–475.
- JEFFERY, G. B. 1915 On the steady rotation of a solid of revolution in a viscous fluid. *Proc. Lond. Math. Soc.* **2**, 327–338.
- KIM, S. & RUSSEL, W. B. 1985 The hydrodynamic interactions between two spheres in a Brinkman medium. *J. Fluid Mech.* **154**, 253–268.
- LUNDGREN, T. S. 1972 Slow flow through stationary random beds and suspensions of spheres. *J. Fluid Mech.* **51**, 273–299.
- O'NEILL, M. E. 1964 A slow motion of viscous liquid caused by a slowly moving solid sphere. *Mathematika* **11**, 67–74.
- O'NEILL, M. E. & BHATT, B. S. 1991 Slow motion of a solid sphere in the presence of a naturally permeable surface. *Q. J. Mech. Appl. Maths* **44**, 91–104.
- SAFFMAN, P. G. 1971 On the boundary condition at the surface of a porous medium. *Stud. Appl. Maths* **1**, 93–101.
- SMITH, M. L., LONG, D. S., DAMIANO, E. R. & LEY, K. 2003 Near-wall μ -PIV reveals a hydrodynamically relevant endothelial surface layer in venules *in vivo*. *Biophys. J.* **85**, 637–645.
- SOLOMENTSEV, Y. E. & ANDERSON, J. L. 1996 Rotation of a sphere in Brinkman fluids. *Phys. Fluids* **8**, 1119–1121.
- STACE, T. M. & DAMIANO, E. R. 2001 An electrochemical model of the transport of charged molecules through the capillary glycocalyx. *Biophys. J.* **80**, 1670–1690.
- STIMSON, M. & JEFFERY, G. B. 1926 The motion of two spheres in a viscous fluid *Proc. R. Soc. Lond.* **3**, 110–116.

- TAM, C. K. W. 1969 The drag on a cloud of spherical particles in low Reynolds number flow. *J. Fluid Mech.* **38**, 537–546.
- TAYLOR, G. I. 1971 A model for the boundary condition of a porous material. Part 1. *J. Fluid Mech.* **49**, 319–326.
- TRUESDELL, C. & TOUPIN, R. 1960 The classical field theories. In *Handbuch der Physik.* (ed. S. Flügge), pp. 226–793. Springer.
- VINK, H. & DULING, B. R. 1996 Identification of distinct luminal domains for macromolecules, erythrocytes, and leukocytes within mammalian capillaries. *Circ. Res.* **79**, 581–589.